Use of Airborne Laser Scanning to assess effects of understorey vegetation structure on nest-site selection and breeding performance in an Australian passerine bird

Richard S. Turner [1,2 *], Ophélie J. D. Lasne [1], Kara N. Youngentob [1,3], Shukhrat Shokirov [1,3], Helen L. Osmond [1], & Loeske E. B. Kruuk [1,2]

[1] Division of Ecology & Evolution, Research School of Biology, Australian National University, Canberra, Australia

[2] Institute of Ecology and Evolution, School of Biological Sciences, University of Edinburgh, Edinburgh, United Kingdom

[3] The Fenner School of Environment & Society, Australian National University, Canberra, Australia

[*] Corresponding author. Email: richard.turner@anu.edu.au

ABSTRACT

In wild bird populations, the structure of vegetation around nest-sites can influence the risk of predation of dependent young offspring, generating selection for breeding birds to choose nest-sites with vegetation characteristics associated with lower predation rates. However, for researchers, vegetation structure can be difficult to quantify objectively in the field, which might explain why there remains a general lack of understanding of which characteristics are most important in determining rates of predation. Airborne Laser Scanning (ALS) offers a powerful means of measuring vegetation structure at unprecedented resolution across different spatial scales. Here, we combined ALS with 11 years of breeding data from a wild population of superb fairy-wrens *Malurus cyaneus* in south-east Australia, a species which nests relatively close to the ground and has high rates of nest and fledgling predation. We derived structural measurements of understorey (0-8 m) vegetation from a contiguous grid of 30 x 30 m resolution cells across our *c.* 65 hectare study area. We tested whether: (i) cells with nests differed in their understorey vegetation structure characteristics compared to those without nests; and (ii) the selection of these sites for nesting was adaptive, by assessing the effects of vegetation characteristics on rates of nest success and fledgling survival, and the subsequent probability of a breeding female having any reproductive success. We found that nest-cells differed from unused cells primarily in having denser vegetation in the lowest layer of the understorey (0-2 m; the 'groundstorey' layer). Understorey vegetation was also on average lower in height in nest-cells. However, relationships between understorey vegetation structure characteristics and breeding performance were mixed. Nest success rates decreased with higher volumes of groundstorey vegetation; as did fledgling survival rates, though only in nest-cells with lower height vegetation. Reproductive success was not influenced by any of the

understorey vegetation structure characteristics considered. Our results therefore indicate that ALS data can identify understorey vegetation structure characteristics relevant for superb fairy-wren nest-site selection, but that nesting preferences are not beneficial under current predation pressures. Overall, our study illustrates the potential of using ALS to investigate how ecological processes affect behaviour and life-histories in wild animal populations.

Keywords: "Active Remote Sensing", "Airborne Laser Scanning", "LiDAR", "Nest-Site Selection", "Vegetation Structure", "Avian Breeding Performance", "Nest Predation", "Malurus cyaneus"

INTRODUCTION

Dependent young offspring of many wild animal populations are frequently vulnerable to predation. The importance of predation of dependent young offspring on the evolution and plasticity of breeding behaviours is increasingly recognised in evolutionary and behavioural ecology (Ibáñez-Álamo et al., 2015; Lima, 2009; Lima & Dill, 1990). Studies of birds provide an excellent system to explore the determinants and consequences of predation of dependent young offspring. The loss to predation of eggs and nestlings in nests (i.e., nest predation) is often the primary determinant of breeding failure (Martin, 1993; Ricklefs, 1969), and evidence suggests that, globally, rates of nest predation have increased in recent decades (Kubelka et al., 2018; Matysioková & Remeš, 2022; Remeš et al., 2012a, 2012b). Even after leaving the nest, fledglings can in some cases suffer 5 – 10% mortality per day, due mostly to predation (Naef-Daenzer & Grüebler, 2016; Naef-Daenzer et al., 2001). Understanding the determinants of nest and fledgling predation is therefore central to understanding the ecological pressures that shape the breeding behaviours and life-histories of birds, including for informing appropriate conservation and management strategies for imperilled species.

The structure of the vegetation surrounding the nest-site can play an important role in determining nest predation and may also similarly affect rates of fledgling predation in species where young are relatively sedentary even after leaving the nest. Two structural vegetation characteristics generally considered to influence nest and fledgling predation, and hence site selection, are vegetation density and vegetation complexity, with denser and more complex vegetation thought to reduce nest and fledgling predation by reducing the transmission of sensory cues (particularly visual and auditory cues) to potential predators (Filliater et al., 1994; Magrath et al., 2010; Martin, 1993; Mouton & Martin, 2019). Denser

and more complex vegetation might also impede predators physically by creating a barrier that reduces their ability to access nests or fledglings or reduce their searching efficiency (Bowman & Harris, 1980; Martin, 1993; Martin & Roper, 1988). Natural selection is therefore expected to favour the selection of sites by breeding individuals, that have more dense and more complex vegetation, especially in systems where the primary predators are visually or auditorily-oriented. However, whilst some studies do show some evidence of reduced rates of nest and fledgling predation in sites with more dense and more complex vegetation, such findings are uncommon (Borgmann & Conway, 2015; Lahti, 2009).

Underlying these findings is the premise that structural vegetation data were measured accurately and precisely. However, manually collecting structural vegetation data in the field is costly and labour intensive, meaning that there is often a trade-off between the level of detail of observation and the size of area that can be surveyed. Most often, studies have based their analyses on structural vegetation data that were visually estimated and taken only within a subset of locations (Borgmann & Conway, 2015), which may be researcher biased and may not provide a realistic representation of the vegetation structure across the broader spatial landscape (Block et al. 1987; Gotfryd & Hansell 1985). For example, a study by Block et al. (1987) found that structural vegetation data estimated visually differed significantly among researchers for 31 of 49 structural vegetation characteristics that they measured, including for 5 of 8 measurements of aspects of vegetation density.

Active remote sensing technology such as Light Detection and Ranging (LiDAR) provides a method for collecting detailed, high-resolution structural vegetation data in a standardised, comparable, and spatially contiguous way (Lefsky et al., 2002; Vierling et al., 2008). LiDAR therefore offers immense potential for overcoming many of the difficulties associated with traditional methods of assessing vegetation structure. A common platform for collecting LiDAR data is Airborne Laser Scanning (ALS), which uses short-range laser pulses to measure the spatial (x, y, z) coordinates of reflective surface objects, from a sensor mounted to a low-flying aircraft. As the exact timing and position of the sensor on the aircraft are known, the distance to each point location of an object can be calculated precisely and a three-dimensional "point cloud" can be derived (Lefsky et al., 2002; Vierling et al., 2008). Additional attributes can be specified for each point during processing (such as point classification, which defines the type of object that reflected the laser pulse), from which many structural vegetation

characteristics can be calculated at either fine (e.g., a grid cell or a radius around a focal observation point) or broader spatial landscapes (Bakx et al., 2019; Davies & Asner, 2014).

Whilst there is growing availability across different countries and regions of high-resolution ALS datasets, few studies have so far used ALS in evolutionary and behavioural ecology, and such studies have most often focused on using ALS-derived measures of vegetation structure to assess differences in species' distributions, richness, and abundances (Ciuti et al., 2017; Davies & Asner, 2014; de Vries et al., 2021; Shokirov et al., 2023). Nevertheless, some recent studies have illustrated the promising potential of combining ALS data with behavioural and life-history data of wild animal populations (e.g., in African wild dogs *Lycaon pictus*, Davies et al., 2016; Bornean orangutans *Pongo pygmaeus*, Davies et al., 2019; great tits *Parus major*, Hill et al., 2004 and Hill & Hinsley, 2015; Siberian jays *Perisoreus infaustus*, Klein et al., 2020). For example, Klein et al. (2020) used structural vegetation characteristics derived from ALS data spanning an area of 8300 hectares to demonstrate that reproductive success of Siberian jays was positively associated with an increased understorey vegetation density in territories close to human settlements, which are an indicator of the occurrence of their main nest predator, the visually-oriented Eurasian jay *Garrulus glandarius*. Their study revealed relationships between structural vegetation characteristics and reproductive success that were likely only possible to discover due to the high-resolution and broad spatial coverage of the ALS data.

Here, we used ALS data in combination with 11 years of breeding data from a long-term study of a wild population of superb fairy-wrens *Malurus cyaneus* in the Australian Capital Territory, Australia. Superb fairy-wrens are facultative cooperative breeders: a territory held by a dominant socially monogamous pair may also contain as many as five additional males (Cockburn et al., 2008; Hajduk et al., 2021). Female superb fairy-wrens are solely responsible for nest-building and incubation, but all group members help defend and provision the brood (Cockburn et al., 2016; Rowley & Russell, 1997). Nests are built close to the ground (typically <2 m, Figure S1) in dense grass tussocks or small shrubs (Figure S2). The species are multi-brooded: the breeding season usually begins in September, at the start of the austral spring, and can last until March of the subsequent calendar year (Lv et al., 2019). High rates of nest (Figure S3) and fledgling (Figure S4) predation mean a female may initiate as many as nine or ten clutches per breeding season, but often only one brood (if any) successfully reaches

113 independence. Clutch sizes can range from one to five eggs, but clutches with three eggs are most
114 common (Cockburn et al., 2016; Rowley & Russell, 1997).
115
116 Superb fairy-wrens have many nest and fledgling predators (Rowley & Russell, 1997). In our study area,
117 known predators include red foxes *Vulpes vulpes*, black rats *Rattus rattus*, common brush-tail possums
118 *Trichosurus vulpecula*, and eastern brown snakes *Pseudonaja textilis* (Turner et al., unpublished data).
119 However, previous studies indicate that the dominant predator in our study area is the pied currawong
120 *Strepera graculina*, a large avian passerine, with the colour bands of superb fairy-wren nestlings and
121 fledglings commonly found in their regurgitated pellets (Prawiradilaga, 1996). Indeed, pied currawongs
122 have been implicated as the dominant predator of most small passerines throughout eastern Australia
123 (Bayly & Blumstein, 2001; Fulton & Ford, 2001; Fulton, 2019).
124
125 Pied currawongs use visual and auditory cues to detect and observe their potential prey. If they detect
126 any activity, they then search the location carefully by walking slowly, frequently stopping, and listening
127 intently with their head lowered towards the ground (Wood, 2000; Yasukawa & Cockburn, 2009). Given
128 this searching method, superb fairy-wrens should be expected to have evolved to favour sites with more
129 dense and more complex vegetation, if these structural vegetation characteristics reduce the
130 detectability and accessibility of nests and fledglings to pied currawongs, as is expected. However,
131 counter to this expectation, a recent study of our population found increased rates of nest predation and
132 decreased numbers of fledglings in territories with increased percentages of midstorey cover, measured
133 visually as the percentage of sky occluded by vegetation at a height ranging from 0.7 – 2.5 m above the
134 ground (Backhouse et al., unpublished data). Similar findings have been documented elsewhere. For
135 example, in a population of superb fairy-wrens in South Australia, rates of nest predation increased
136 with the percentage of nest concealment, measured visually as the percentage of vegetation immediately
137 surrounding the nest (Colombelli-Négrel & Kleindorfer, 2009). However, in a population of superb
138 fairy-wrens in New South Wales, Nias (1986) found that nest success rates increased with concealment;
139 although, in this study, nests that were considered more concealed were mostly built in non-native
140 *Rubus vulgaris* brambles that contain protective thorns, which might have deterred predators. Of these
141 three studies, none found evidence of any other structural vegetation characteristics influencing rates
142 of nest or fledgling predation. However, in each study, structural vegetation data were estimated
143 visually, from within a subset of locations, and measures were summarised into relatively course and

arbitrary categories. Moreover, neither study tested whether the same characteristics were also important for nest-site selection – for example, by comparing whether sites containing nests differed in their structural vegetation characteristics versus sites without nests.

In this study, we used high-resolution ALS data to derive three key vegetation structure characteristics related to the vegetation height, complexity, and density (defined in Table 1) from a contiguous grid of 30 x 30 m resolution cells spanning the extent of our study area. We focused on quantifying aspects of the vegetation structure in only the understorey (0 – 8 m; details below) because superb fairy-wrens generally nest relatively close to the ground (Figure S1; Cockburn et al., 2016; Rowley & Russell, 1997), and as such we expected that the structure of the understorey vegetation would be most important in determining site selection and breeding performance for this species. We tested: (i) whether our three understorey vegetation structure characteristics influenced site selection; and (ii) whether site selection was adaptive in relation to predation, by assessing the effects of these characteristics on seasonal rates of nest success and fledgling survival, and the subsequent probability of reproductive success (defined in Table 2).

2 | MATERIALS AND METHODS

2.1 | Study area

The study area is located in Canberra, Australian Capital Territory, Australia (Figure 1) and encompasses an area of *c.* 65 hectares that includes a *managed* area (*c.* 43 hectares) in the Australian National Botanic Gardens (ANBG) and an *unmanaged* area (*c.* 22 hectares), which is part of the adjacent Black Mountain Nature Reserve. The study area is broadly characterised as mature open sclerophyll forest, with the primary tree species including evergreen *Eucalyptus macrorhyncha* and *Eucalyptus rossii*. Shrubs and grasses including *Acacia* spp.*, Callistemon* spp.*, Notodanthonia* spp., *Rytidosperma palladium*, *Triodia scariosa,* and *Lomandra longifolia* are dominant through the understorey. The *managed* area further consists of a diverse collection of native vegetation established within dense plantings, and three semi-artificial habitats (specifically, a 'rainforest' area, a 'desert' area, and a grass lawn). Along a small patch of the eastern perimeter of the *unmanaged* area, a collection of gullies has formed, which sometimes flood with rainwater. Much of this patch is dominated by *Bursaria spinosa* and other swamp specialists, and non-native species including *Rubus fruticosus* spp (Fraser & Purdie, 2020).

Two large hailstorms damaged much of the study area on 27 February 2007 and 19 January 2020. In this study, we therefore constrained our analyses to observations from 11 breeding seasons (from 2009/10–2019/20; up until the hailstorm on 19 January 2020), centred around 2015/2016 when the ALS data were collected (details below). Hereafter, we refer to a given breeding season by the calendar year in which it commenced. The weather conditions were relatively constant across this time (Figure S5) and the general structure of the vegetation remained largely unchanged. As a result, we did not expect any time difference between the superb fairy-wren breeding data and the ALS survey to affect our ability to detect any relationships (Hill & Hinsley, 2015; Vierling et al., 2014). For completeness, we also repeated all analyses using data from 1994 – 2019 (which is the duration for which comprehensive superb fairy-wren breeding data have been collected across the full extent of our study area) and found effectively identical results, which we present separately in Table S1.

2.2 | Superb fairy-wren breeding data collection and processing

Between 2009 – 2019, the study area supported between 34 – 79 superb fairy-wren territories each year, with an average territory size of 1.09 ± 0.71 hectares (mean ± SD, n = 686 territory-years). Individuals in the study population were uniquely colour-banded, allowing for individual recognition.

During the breeding season, we located nests by observing the breeding female during nest-building or by following them to the nest during incubation. The location of each nest was recorded using Global Positioning System (GPS) with ± 3 m resolution. The progress of each nest was monitored every second day for the duration of the nesting period (typically 24 days from the onset of incubation) to determine *nest fate*. Nests that fledged at least one offspring were considered *successful*. Predation of the nest was assumed when all eggs or nestlings disappeared prior to their expected fledging date. Because our interest was in whether site selection influenced breeding performance via predation risk, we excluded 172 nests (9.35% of the total) that failed due to reasons other than predation (Figure S3). In cases where nests were successful, we closely monitored individual fledglings to determine their survival to independence, defined as four weeks (28 days) post-fledging. Although most offspring are still being provisioned at this age, five-weeks post-fledging is the earliest known age of dispersal in our study area; our four-week cut-off point therefore avoids any chance of dispersal being confused with mortality (Hajduk et al., 2018, 2020). Causes of fledgling mortality are generally unknown, but the recovery of

colour bands of fledglings from pellets of pied currawongs suggests that predation is an important source of mortality (Prawiradilaga, 1996). In this study, we used all fledgling mortality as a measure of fledgling predation.

Following Backhouse et al. (unpublished data), we derived measurements of understorey vegetation structure from a contiguous grid of 30 x 30 m resolution cells (n = 768 cells) spanning the extent of our study area (details below). Because superb fairy-wren territories were on average 1.09 hectares in size, each 30 x 30 m resolution cell encompassed *c.* 10% of the average territory. To match superb fairy-wren breeding data to the same spatial scale as the understorey vegetation structure data, we assigned each nest to a cell based on their GPS coordinates. At this point of data processing, we excluded breeding data from 25 cells (3.3% of the total) that encompassed the three semi-artificial habitats in the study. We have shown previously that superb fairy-wrens do not inhabit these regions of our study area because they contain vegetation that is very different from their native range (Backhouse et al., unpublished data). Breeding data from a further two cells were later excluded as they contained no understorey vegetation structure data (details below).

The final superb fairy-wren breeding dataset used in this study comprised of observations from a total of 1431 nests (from 318 breeding females), encompassing 741 cells over 11 years (n = 8151 cell-years). For analysis of nest-site selection, cell-years were subsequently further designated as nest-cell-years (i.e., cell-years with a nest, n = 1094 cell-years) or unused cell-years (i.e., cell-years without a nest, 7057 cell-years). For each nest-cell-year we considered the following three measures of breeding performance: nest success rate, fledgling survival rate, and reproductive success (defined in Table 2). Note that in rare cases, it is possible for more than one breeding female to occupy a given nest-cell-year – for example, in cases where cells overlapped territory boundaries, or the death of a breeding female resulted in her being replaced. In these cases, observations were treated as independent for each breeding female (i.e., female-nest-cell-year).

The number of cells with a nest declined significantly over the course of the study (Figure S6a), a finding that is consistent with the observation of a 72.16% population decline of breeding females during the period considered here (Figure S6b), and with a general decline across the entire study period (Backhouse et al, unpublished data). The decline in population size may be linked to increased rates of

adult winter mortality associated with climate change (Lv et al, in press). For the purpose of this study, we do not focus on this decline in detail.

2.2 | Airborne Laser Scanning data collection and processing

ALS data were collected between 21 May 2015 and 5 April 2016 and were obtained from the Australian Capital Territory Government's Environment, Planning and Sustainable Development Directorate (www.planning.act.gov.au, obtained 23 June 2021). The data were recorded as part of a regional survey, using an AX60 scanner mounted to an aircraft (with a Riegl LMS-Q780 sensor and Trimble AP50 GPS). Details of the ALS survey were as follows: flight elevation above ground level: 450 m; point density: 8 pulses/m^2; footprint size: 0.12 m; swath width: 539 m; overlap: 25%; vertical precision: ± 0.30 m; horizontal precision: ± 0.80 m. Further details including the flight speed, laser wavelength, scan frequency, and pulse frequency were not provided with the dataset (www.planning.act.gov.au). The raw ALS data was pre-processed by the vendor and came with a classification of *ground*, *building*, *water*, *vegetation*, and *noise* points. The data were distributed in LAS v.1.4 format projected in spatial reference Geocentric Datum of Australia 1994, Map Grid of Australia Zone 55 (www.planning.act.gov.au).

We separated the raw ALS data into each of our 30 x 30 m resolution cells using LAStools (rapidlasso GmbH; van Rees, 2013). We used the package 'lidR' (v.3.1.3; Roussel et al., 2020) in R (v.4.0.5; R Core Team, 2021) to further process the ALS data and derive vegetation structure characteristics for each cell as follows: First, point cloud data were normalised by subtracting the height of ground points from the height of non-ground points (following e.g., Ciuti et al., 2018; Korma et al., 2021; Roussel et al., 2020; Shokirov, 2021; Shokirov et al., 2023). Second, points classified as *ground*, *building*, *water*, and *noise* were removed, resulting in only points classified as *vegetation* being retained. A total of two cells were found to contain no *vegetation* points, and so at this stage they were excluded from further processing. Third, *vegetation* points were reclassified into two layers: *understorey layer* (0 – 8 m), and *canopy layer* (> 8 m). We used 8 m as the threshold distinguishing these two vegetation layers based on the distribution of the *z* coordinates (i.e., height values) of the point cloud (Figure S7) and detailed knowledge of the primary *Eucalyptus* spp. in the study area (Fraser & Purdie, 2020). We then removed *canopy vegetation* points from the point cloud data as we expected the structure of the understorey vegetation to be most relevant for superb fairy-wrens based on their nesting behaviour (Figure S1–S2).

Fourth, from the *understorey vegetation* points, we calculated three vegetation structure characteristics related to aspects of the vegetation height, complexity, and density that are most often used in studies aiming to understand the determinants and consequences of nest-site selection in birds (Borgmann & Conway, 2015; Filliater et al., 1994). The three characteristics we calculated were: *mean height* of the understorey vegetation, *variation in height* of the understorey vegetation (as measured by the standard deviation, SD) and *volume* of the understorey vegetation. We initially calculated *volume* within four specific height thresholds (0 – 2 m, 2 – 4 m, 4 – 6 m, 6 – 8 m) but because the nests of superb fairy-wrens are generally <2 m above the ground, in our analyses we considered *volume* at the lowest height threshold only (hereafter referred to as '*groundstorey volume*'). Definitions of each of the three understorey vegetation structure characteristics are provided in Table 1. The final ALS point cloud dataset used in this study comprised a total of 1,686,744 understorey vegetation points, with a mean ± SD of 2270.18 ± 1994.04 points/cell.

2.3 | Statistical analysis

Analyses were conducted using a Bayesian framework implemented in the package 'brms' (v.2.15.0; Bürkner, 2017) in R (v.4.0.5; R Core Team, 2021). Prior to analysis we mean standardised all explanatory parameters to allow for effect size comparisons (Harrison et al., 2018; Schielzeth, 2010). We assessed potential multicollinearity between explanatory parameters for each dataset by checking variance inflation factors (VIF), using the *check_collinearity* function in the package 'performance' (v.0.7.2; Lüdecke et al., 2021), and by conducting Pearson correlation tests. All VIF factors were < 2.10 and all correlation coefficients were < 0.45, indicating that explanatory variables were not strongly correlated with each other (Table S2–S3; Dormann et al., 2013, Zuur et al., 2009). Additionally, we assessed potential spatial autocorrelation among our understorey vegetation structure parameters by calculating Moran's *I* statistic (Moran, 1950), using the *moran.mc* function in the package 'spdep' (v.1.1.8; Bivand et al., 2013). We found evidence of spatial clustering in our datasets (Figure S8, Table S4: i.e., cells that were close together were more similar in their vegetation structure than sites further apart). We therefore included a spatial conditional autoregressive (CAR) structure in our models (Figure S9) to account for this spatial autocorrelation (Bürkner, 2017; Dormann et al., 2007; Ciuti et al., 2017; Zuur et al., 2009). Further details are provided as Appendix S1 in Supplementary Information.

298 We constructed Bayesian spatial hierarchical generalised linear regression models for each of our four
299 response variables of nest presence, nest success rate, fledgling survival rate, and reproductive success
300 (Table 2). In all models, we included fixed effects of year (as a continuous covariate) plus the three
301 understorey vegetation structure parameters. To account for repeated measurements of non-
302 independent data, we included cell ID and year (as multi-level factors) as random effects in all models.
303 Female ID was additionally included as a random effect in the three models of breeding performance to
304 account for multiple observations of the same breeding female.
305
306 We initially also considered: non-linear (i.e., quadratic) effects of all understorey vegetation structure
307 parameters; the two different parts of the study area (as a two-level factor: managed, unmanaged); and
308 possible two-way interactions between all explanatory parameters. In cases where these effects were
309 non-significant, we discarded them from our final models (and do not present them here). Previous
310 studies of superb fairy-wrens have shown positive associations between a female's age, the number of
311 helpers, and a suite of breeding performance metrics (e.g., Cockburn *et al.,* 2008; Hajduk et al., 2020,
312 2021). We therefore included as fixed effects female age (as a two-level factor: 1 year old, 2+ year old,
313 following e.g., Backhouse et al., unpublished data; Kruuk et al., 2015; Hajduk et al., 2018) and number
314 of helpers (as a two-level factor: 0 helpers, 1+ helpers, following e.g., Cooper et al., 2020; Taylor &
315 Langmore, 2020) in our three models of breeding performance to control for their effects, but we do
316 not focus on these effects in detail in our results because the focus of this study was to examine the
317 effects of understorey vegetation structure on nest-site selection and breeding performance.
318
319 We ran all models on 4 independent MCMC chains for 8000 iterations, with a thinning interval of 10
320 and a warm-up period of 3000 iterations (resulting in a total of 2000 posterior samples), specifying
321 weakly informative priors with a normal error distribution (μ: 0; σ^2: 1; Gelman et al., 2015). The effective
322 sample sizes for specific parameters varied owing to autocorrelation, but we ensured that they were
323 always above 400 (i.e., a minimum effective sample size of 100 per chain; Vehtari et al., 2021). Model
324 convergence was confirmed visually by inspecting the trace plots of parameter estimates, and by
325 ensuring that potential scale reduction factors were < 1.01 (Gelman et al., 2013; Vehtari et al., 2021).
326 For each model, we assessed the goodness-of-fit using the posterior predictive check, *pp_check*,
327 function in the package 'bayesplot' (v.1.8.1; Gabry & Mahr, 2021). Unless stated otherwise, summary
328 statistics are presented as means (± SE). Model parameter estimates are presented as posterior means

(± SD) and 95% credible intervals. We consider there to be statistical support for specific parameters when the 95% credible intervals do not span zero.

RESULTS

Understorey vegetation structure parameters

The mean (± SD) of the three understorey vegetation structure parameters were as follows: mean height: 3.3 ± 1.0 m (Figure 2c); SD height: 2.2 ±0.4 m (Figure 2d); groundstorey volume: 378.4 ± 267.8 m^3 (Figure 2e). There was a positive correlation between mean height and SD height (Pearson correlation coefficient = 0.30), and negative correlations between mean height and groundstorey volume (Pearson correlation coefficient = -0.42) and between SD height and groundstorey volume (Pearson correlation coefficient = -0.25) (Table S3).

Nest-site selection

Of the 741 cells, 39.41% (n = 292 cells) never had a nest during the 11 years of our study, while 23.35% (n = 173 cells) had a nest in 1 year only (Figure 1, Figure S10). The maximum number of years a cell had a nest was 9 years (two cells; Figure 1).

In relation to the understorey vegetation structure, the probability of nest presence in a cell decreased with increasing mean height (nest-cell-years: 3.01 ± 0.03 m; unused cell-years: 3.33 ± 0.01 m; Table 3, Figure 3a – b), and increased with increasing groundstorey volume (nest-cell-years: 477.20 ± 8.53 m^3; unused cell-years: 363.09 ± 3.12 m^3; Table 3, Figure 3c – d). Note that because a cell encompasses *c.* 10% of the average superb fairy-wren territory, random nest-site selection within a territory would be expected to predict an average probability of 0.10 for nest presence. Rates of nest presence >0.10 therefore indicate preference for sites with lower (Figure 3b) and denser vegetation (Figure 3d). We found no significant effect of SD height on nest presence (Table 3).

Nest success rate

The nest success rate was on average 0.44 ± 0.01 (n = 1138 female-nest-cell-years) and varied between years. The highest nest success rate occurred in 2012 (0.51 ± 0.04; 123 female-nest-cell-years), while the lowest nest success rate occurred in 2019 (0.36 ± 0.07; n = 50 female-nest-cell-years). We found no significant linear change of nest success rate over time (Table 3). Most often cells contained only one

nest from one female only in a given year (80.84% female-nest-cell-years; range 1 – 4). As such, nest success rates were generally either 0.00 (51.41%; n = 585 female-nest-cell-years) or 1.00 (39.81%; n = 453 female-nest-cell-years).

We found no effect of mean height on nest success rate (female-nest-cell-years in which nest success rate > 0.00: 3.00 ± 0.04 m; female-nest-cell-years in which nest success rate was 0.00: 3.02 ± 0.03; Table 3, Figure 4a–b). Similarly, we found no effect of SD height on nest success rate (Table 3). However, there was a significant decline in nest success rate with increasing groundstorey volume (female-nest-cell-years in which nest success rate > 0.00: 463.96 ± 11.39 m^3; female-nest-cell-years in which nest success rate was equal to 0.00: 490.16 ± 12.07; Table 3, Figure 4c–d).

Fledgling survival rate

Fledgling survival rate was on average 0.61 ± 0.02 (n = 556 female-nest-cell-years). The highest fledgling survival rate occurred in 2016 (0.76 ± 0.04; n = 53 female-nest-cell-years), whilst 2013 had the lowest fledgling survival rate (0.50 ± 0.05; n = 57 female-nest-cell-years). The average number of fledglings produced across all female-nest-cell-years was 2.96 ± 0.05 (range: 1 - 9), which corresponds to the typical clutch size of three eggs (Cockburn et al., 2016; Rowley & Russell, 1997).

None of the understorey vegetation structure parameters were significant as main effects for fledgling survival rate (Table 3). However, we did find a significant interaction between mean height and groundstorey volume: fledgling survival rates decreased with groundstorey volume when female-nest-cell-years contained smaller understorey vegetation (i.e., when mean height was lower than the population-level average, n = 268 female-nest-cell-years; Table 3, Figure 5).

Reproductive success

A total of 37.70% female-nest-cell-years produced one or more independent offspring overall (n = 429 of 1138 female-nest-cell-years). The highest percentage of female-nest-cell-years to produce independent offspring occurred in 2018 (45.33%; n = 34 of 75 female-nest-cell-years) and 2012 (43.09%; n = 53 of 123 female-nest-cell-years), while the lowest percentage of female-nest-cell-years to produce independent offspring occurred in 2019 (26.00%; n = 13 of 50 female-nest-cell-years). None of

the understorey vegetation structure parameters were found to significantly influence whether a female had any reproductive success in a nest-cell in a given year (Table 3).

DISCUSSION

Our study combined high-resolution ALS-derived measures of understorey vegetation structure with detailed breeding data from a long-term study of a population of superb fairy-wrens. We found differences in the characteristics of understorey vegetation structure in sites chosen for nesting, but no evidence that this selection reduced the risk of nest or fledgling predation. We discuss the outcomes of these results in turn below, and the implications for the use of ALS in studies of the evolutionary and behavioural ecology of wild animal populations.

Understorey vegetation structure characteristics and nest-site selection

Our results indicate that female superb fairy-wrens select where to build their nests and raise their offspring based on aspects of the understorey vegetation height, complexity, and density. The probability of nest presence in a given 30 x 30 m resolution cell increased with decreasing mean height of the understorey vegetation in that cell. A low mean height value is indicative of an area containing more grass tussocks and small shrubs, vegetation types that superb fairy-wrens preferentially use to nest in within our study area (Figure S2). Nest presence also increased with groundstorey volume, with nest-cells having a higher value of groundstorey volume compared to unused cells. We found no statistical significance of SD height affecting the probability of nest presence. However, this was possibly due to a lack of power in the 11 year subset of data (i.e., 2009 – 2019) used in this analysis; when we repeated our nest presence analyses using the full dataset (i.e., 1994 – 2019), we found that the parameter estimates were almost identical, but reduced error around the estimate meant that the positive association between SD height and nest presence was statistically significant (Table S1). Denser and more complex vegetation, particularly immediately surrounding the nest, is expected to be favoured in response to a preponderance of visually and auditorily-oriented predators (Bowman & Harris, 1980; Martin, 1993; Martin & Roper, 1988; Filliater et al., 1994). Our results are therefore consistent with the expectation that superb fairy-wrens' choice of where to nest and raise their offspring is shaped by predation pressures.

Vegetation structure characteristics and superb fairy-wren breeding performance

Previous studies of superb fairy-wrens have reported increased rates of nest predation and decreased numbers of fledglings in relation to visually estimated aspects of vegetation density (Backhouse et al., unpublished data; Colombelli-Négrel & Kleindorfer, 2009). Our study confirms these findings when measuring vegetation density from high-resolution ALS data by showing that nest success rates decreased with increasing volume of groundstorey-level vegetation. Fledgling survival rates also decreased with increasing groundstorey volume, though only when the mean height was lower. Overall, groundstorey volume did not significantly affect whether a female achieved any reproductive success in a given 30 x 30 m resolution nest-cell. As before, this finding was possibly due to a lack of power in the subset of data used in this study; when we repeated our reproductive success analyses using the full dataset, we found almost identical effect sizes, but the negative groundstorey volume effect was significant due to reduced error with the larger sample sizes (Table S1). Our findings therefore indicate a potential paradox: why do nest-sites with increased groundstorey volume have decreased rates of nest success and fledgling survival when such structural vegetation characteristics should be adaptive against visually and auditorily-oriented predators, such as pied currawongs?

There are several possible explanations for this paradox. Whilst pied currawongs have been previously identified as the dominant species responsible for depredating the nests and fledglings of superb fairy-wrens in our study population (Prawiradilaga, 1996), they were not present in our study area until the 1970s (Taylor, 1992). It is therefore possible that superb fairy-wren nest-site selection evolved in response to historical selection pressures generated by different predatory species (Chalfoun & Schmidt, 2012), with pied currawongs not deterred by dense vegetation, and hence current nest-site preferences are insufficient at impeding the pied currawong's ability to detect and access the nests and fledglings of superb fairy-wrens.

Alternatively, superb fairy-wren nest-site selection might be adaptive against pied currawongs, but the current importance of pied currawongs as a predator of superb fairy-wren nests and fledglings in our study area may have been overestimated, or the dynamics between superb fairy-wrens and pied currawongs may have changed since Prawiradilaga (1996). Indeed, despite a sustained increase in the numbers of pied currawongs in our study area (Cockburn, unpublished data), long-term rates of superb fairy-wren nest predation have decreased (Table S1; Backhouse et al., unpublished data).

452 It is also possible that nesting in areas with increased groundstorey volume may make superb fairy-
453 wren nests and fledglings more vulnerable to other predators (Filliater et al., 1994). Red foxes are also
454 common predators of superb fairy-wren nests and fledglings in our study area (Turner et al.,
455 unpublished data). Elsewhere in Australia, red foxes have been linked to the extinction of an estimated
456 14 native mammal species and one bird species (Woinarski et al. 2019), and to the ongoing population
457 declines of many others (Woinarski et al. 2022), because of their generalist diet and ability to thrive in
458 a range of habitat types. Red foxes often locate their prey using olfactory cues, which may not be reduced
459 by structural vegetation characteristics (Colombelli-Négrel & Kleindorfer, 2009). It is therefore possible
460 that current nest-site preferences are not adaptive to predation pressures imposed by red foxes. In our
461 study, we do not have sufficient observations of predation events to test whether the relative importance
462 of understorey vegetation structure on superb fairy-wren breeding performance differed with predator
463 species, but our results illustrate the need to understand the potential importance of other predators.
464
465 *Potential use and limitations of ALS in future studies in evolutionary and behavioural ecology*
466 Few studies have so far used ALS in evolutionary and behavioural ecology, and such studies have most
467 often focused on using ALS-derived measures of vegetation structure to assess differences in species'
468 distributions, richness, and abundances (Ciuti et al., 2017; Davies & Asner, 2014; de Vries et al., 2021;
469 Shokirov et al., 2023). In general, these studies have found significant (positive or negative) associations
470 between one or more ALS-derived measures of vegetation structure and these different components of
471 species composition (Davies & Asner, 2014), including in a landscape with a very similar vegetation
472 structure to our study area (Shokirov et al., 2023). More recently, studies have also shown that ALS data
473 can be used to assess how structural vegetation characteristics affect the breeding behaviours and life-
474 histories of single populations or species (Davies et al., 2016, 2019; Hill et al., 2004; Hill & Hinsley,
475 2015; Klein et al., 2020). Much of these studies have thus far been conducted in North America and
476 Europe and are biased towards a few taxonomic groups, mainly birds (Davies & Asner, 2014). However,
477 the increasing accessibility of national or regional ALS datasets means there is tremendous potential
478 for studies to be conducted globally for entire taxonomic groups and ecosystems (Lefsky et al. 2002,
479 Vierling et al. 2008).
480
481 While traditional field methods can also be used to assess vegetation structure, doing so may be costly,
482 labour intensive and more subjective, and measurements are usually only taken at a subset of locations.

Obtaining structural vegetation data in remote environments or across rugged terrains can also be particularly challenging. In contrast, ALS can produce spatially contiguous measures of vegetation structure at high resolution, thereby producing a more realistic representation of vegetation structure of the landscape. ALS also provides a means of collecting data in areas that have restricted or limited access, and to cover broad spatial extents that would otherwise be impossible using traditional field methods. It should be noted that several previous studies have found strong associations between structural vegetation characteristics derived from ALS and those measured quantitatively in the field (Hyde et al., 2005, 2006). However, one advantage of ALS is that it allows for more complex measures of vegetation structure to be calculated (Bakx et al., 2019). Additionally, these calculations can be done post-hoc, as our understanding of the relative importance of different vegetation structural parameters improves.

There are of course limitations to ALS that need to be considered. First, ALS datasets can be computationally demanding, requiring large amounts of computer memory to process. For example, the unprocessed ALS data for our study area (*c.* 65 hectares) was *c.* 10 GB in size and initially consisted of *c.* 250 million data points. Some level of specialisation is also required to process and analyse ALS data, but the development of packages and workflows in geographic information system (GIS) or open-source software such as R and Python has reduced technical challenges (van Rees, 2013; Roussel et al., 2020). Second, the general purpose of many ALS surveys is to provide accurate and precise mapping of the ground terrain (Reutebach et al., 2005). For this reason, most ALS surveys are conducted in winter when deciduous trees and shrubs have no leaves to limit introduced 'noise' from vegetation points. ALS data captured in winter may thus not provide a realistic representation of vegetation structure for landscapes in which deciduous species are abundant. Future studies are needed to understand the effect of seasonality on the ability of ALS to accurately capture structural vegetation data. Note, however, the vegetation in our study area is predominantly evergreen, dominated by *Eucalyptus* species (Fraser & Purdie, 2020). Finally, ALS may be ineffective at penetrating through the particularly dense canopy vegetation (Bakx et al., 2019), thus limiting its ability to accurately capture the structural characteristics of understorey vegetation in some landscapes. However, Shokirov et al. (2023) have shown that ALS is effective at capturing understorey vegetation in a landscape close to and similar in structure to our study area, by comparing structural vegetation characteristics derived from ALS and higher resolution Terrestrial Laser Scanning (TLS) and relating these measures to avian species diversity and abundance.

CONCLUSION

Our analysis used ALS to investigate breeding behaviour in a wild bird population, illustrating the specific aspects of the understorey vegetation structure associated with superb fairy-wrens' choice of nest-site. The relationships between understorey vegetation structure and superb fairy-wren breeding performance are complex and highlight the need for future research to consider the relative importance of specific predators. Our study demonstrates the promising potential for using ALS-derived measures of vegetation structure, and in particular for testing effects of more complex measures such as variation in structure, in studies of evolutionary and behavioural ecology. The increasing availability of ALS data provides an exciting opportunity for furthering our understanding of the ecological pressures that shape the breeding behaviours and life-histories of birds, and other wild animal populations, at an unprecedented resolution and spatial coverage.

ACKNOWLEDGEMENTS

We thank Andrew Cockburn for the superb fairy-wren breeding dataset and for discussion and comments on the manuscript. We also thank the many field assistants who have contributed to the study over the years. We thank the Australian National Botanic Gardens for permission to work at the study site (Permit Number: 2013/14-1) and for logistical support, and to the Australian Research Council for long-term funding, of which the latest grant for data used in this study was DP190100424. Ethics approval was granted by the Australian National University Animal Experimentation Ethics Committee (Protocol Number: A2019/23). RST was funded through an Australian National University Research Scholarship (7382018) and HDR Fee Merit Scholarship (3202015) and LEBK was funded by an Australian Research Council Laureate Fellowship (FL200100068) and a Royal Society Research Professorship. We wish to acknowledge the Ngunnawal people, the traditional custodians of the land upon which our study was undertaken. We pay our respects to their Elders, past, present, and emerging.

REFERENCES

Bakx, T.R.M., Koma, Z., Seijmonsbergen, A.C., & Kissling, W.D. (2019). Use and categorisation of light detection and ranging vegetation metrics in avian diversity and species distribution research. *Diversity and Distributions*, *25*, 1045–1059.

544 Bayly, K.L., & Blumstein, D.T. (2001). Pied currawongs and the decline of native birds. *Emu, 101,* 199–
545 204.

546 Béland, M., Baldocchi, D.D., Widlowski, J.L., Fournier, R.A., & Verstraete, M.M. (2014). On seeing the
547 wood from the leaves and the role of voxel size in determining leaf area distribution of forests with
548 terrestrial LiDAR. *Agricultural and Forest Meteorology*, *184*, 82–97.

549 Bivand, R.S., Pebesma, E. & Gomez-Rubio, V. (2013). Applied spatial data analysis with R (2nd edition).
550 Springer, New York, USA.

551 Block, W.M., With, K.A., & Morrison, M.L. (1987). On measuring bird habitat: Influence of observer
552 variability and sample size. *The Condor*, 89, 241–251.

553 Borgmann, K.L., & Conway, C.J. (2015). The nest-concealment hypothesis: New insights from a
554 comparative analysis. *The Wilson Journal of Ornithology*, *127*, 646–660.

555 Bowman, G.B., & Harris, L.D. (1980). Effect of spatial heterogeneity on ground-nest depredation. *The*
556 *Journal of Wildlife Management*, *44*, 806–813.

557 Bürkner, P.C. (2017). brms: An R package for Bayesian multilevel models using Stan. *Journal of*
558 *Statistical Software* 80, 1–28.

559 Chalfoun, A.D., & Schmidt, K.A. (2012). Adaptive breeding-habitat selection: Is it for the birds? *The*
560 *Auk*, *129*, 589–599.

561 Ciuti, S., Tripke, H., Antkowiak, P., Gonzalez, R.S., Dormann, C.F., & Heurich, M. (2018). An efficient
562 method to exploit LiDAR data in animal ecology. *Methods in Ecology and Evolution*, *9*, 893–904.

563 Cockburn, A., Brouwer, L., Margraf, N., Osmond, H.L. & van de Pol, M. (2016). Superb fairy-wrens:
564 Making the worst of a good job. In: Koenig, W.D. & Dickinson, J.L. (Eds). Cooperative Breeding in
565 Vertebrates: Studies of Ecology, Evolution, and Behaviour, pp. 133–149. Cambridge University Press,
566 Cambridge, UK.

567 Cockburn, A., Osmond, H.L., Mulder, R.A., Green, D.J., & Double, M.C. (2003). Divorce, dispersal and
568 incest avoidance in the cooperatively breeding superb fairy-wren *Malurus cyaneus*. *Journal of Animal*
569 *Ecology, 72*, 189–202.

570 Cockburn, A., Sims, R.A., Osmond, H.L., Green, D.J., Double, M.C., & Mulder, R.A. (2008). Can we
571 measure the benefits of help in cooperatively breeding birds: The case of superb fairy-wrens *Malurus*
572 *cyaneus*? *Journal of Animal Ecology*, *77*, 430–438.

573 Colombelli-Négrel, D., & Kleindorfer, S. (2009). Nest height, nest concealment, and predator type
574 predict nest predation in superb fairy-wrens (*Malurus cyaneus*). *Ecological Research*, *24*, 921–928.

575 Cooper, E.B., Bonnet, T., Osmond, H.L., Cockburn, A., & Kruuk, L.E.B. (2020). Do the ages of parents
576 or helpers affect offspring fitness in a cooperatively breeding bird? *Journal of Evolutionary*
577 *Biology*, *33*, 1735–1748.

578 Davies, A.B., & Asner, G.P. (2014). Advances in animal ecology from 3D-LiDAR ecosystem mapping.
579 *Trends in Ecology & Evolution*, *29*, 681–691.

580 Davies, A.B., Marneweck, D.G., Druce, D.J., & Asner, G.P. (2016). Den site selection, pack composition,
581 and reproductive success in endangered African wild dogs. *Behavioural Ecology*, *27*, 1869–1879.

582 Davies, A.B., Oram, F., Ancrenaz, M., & Asner, G.P. (2019). Combining behavioural and LiDAR data to
583 reveal relationships between canopy structure and orangutan nest site selection in disturbed forests.
584 *Biological Conservation*, *232*, 97–107.

585 de Vries, J.P.R., Koma, Z., de Vries, M.F.W., & Kissling, W.D. (2021). Identifying fine-scale habitat
586 preferences of threatened butterflies using airborne laser scanning. *Diversity and Distributions*, *27*,
587 1251–1264.

588 Dormann, C.F., Elith, J., Bacher, S., Buchmann, C., Carl, G., Carré, G., Marquéz, J.R.G., Gruber, B.,
589 Lafourcade, B., Leitão, P.J., Münkemüller, T., McClean, C., Osborne, P.E., Reineking, B., Schröder, B.,
590 Skidmore, A.K., Zurell, D., & Lautenbach, S. (2013). Collinearity: A review of methods to deal with it
591 and a simulation study evaluating their performance. *Ecography*, *36*, 27–46.

592 Dormann, C.F., McPherson, J.M., Araújo, M.B., Bivand, R., Bolliger, J., Carl, G., Davies, R.G., Hirzel,
593 A., Jetz, Kissling, W.D., Kühn, I., Ohlemüller, R., Peres-Neto, P.R., Reineking, B., Schröder, B., Schurr,
594 F.M., & Wilson, R. (2007). Methods to account for spatial autocorrelation in the analysis of species
595 distributional data: A review. *Ecography*, *30*, 609–628.

596 Elmberg, J., Folkesson, K., Guillemain, M., & Gunnarsson, G. (2009). Putting density dependence in
597 perspective: Nest density, nesting phenology, and biome, all matter to survival of simulated mallard
598 *Anas platyrhynchos* nests. *Journal of Avian Biology*, *40*, 317–326.

599 Filliater, T.S., Breitwisch, R., & Nealen, P.M. (1994). Predation on northern cardinal nests: Does choice
600 of nest site matter? *The Condor*, *96*, 761–768.

601 Fulton, G.R. (2019). Meta-analyses of nest predation in temperate Australian forests and woodlands.
602 *Austral Ecology*, *44*, 389–396.

603 Fulton, G.R., & Ford, H.A. (2001). The pied currawong's role in avian nest predation: A predator
604 removal experiment. *Pacific Conservation Biology*, *7*, 154–160.

605 Fraser, I. & Purdie, R. (2020). Black Mountain: A natural history of a Canberra icon. Friends of Black
606 Mountain, Canberra, Australia.

607 Gabry, J., & Mahr, T. (2021). bayesplot: Plotting for Bayesian models. R package version 1.8.1. Available
608 from: https://mc-stan.org/bayesplot.

609 Gelman, A., Carlin, J.B., Stern, H.S., Dunson, D.B., Vehtari, A., & Rubin, D.B. (2013). Bayesian data
610 analysis (3rd edition). Chapman & Hall/CRC Press, London, UK.

611 Gelman, A., Lee, D. & Guo, J. (2015). Stan: A probabilistic programming language for Bayesian
612 inference and optimization. *Journal of Educational and Behavioural Statistics, 40,* 530–543.

613 Gotfryd, A., & Hansell, R.I.C. (1985). The impact of observer bias on multivariate analyses of vegetation
614 structure. *Oikos, 45*, 223–234.

615 Hajduk, G.K., Cockburn, A., Margraf, N., Osmond, H.L., Walling, C.A., & Kruuk, L.E.B. (2018).
616 Inbreeding, inbreeding depression, and infidelity in a cooperatively breeding bird. *Evolution*, *72*, 1500–
617 1514.

618 Hajduk, G.K., Walling, C.A., Cockburn, A., & Kruuk, L.E.B. (2020). The 'algebra of evolution': The
619 Robertson-Price identity and viability selection for body mass in a wild bird population. *Philosophical*
620 *Transactions of the Royal Society B: Biological Sciences,* 375, 20190359.

621 Hajduk, G.K., Cockburn, A., Osmond, H.L. & Kruuk, L.E.B. (2021). Complex effects of helper
622 relatedness on female extrapair reproduction in a cooperative breeder. *Behavioural Ecology*, *32*, 386–
623 394.

624 Harrison, X.A., Donaldson, L., Correa-Cano, M.E., Evans, J., Fisher, D.N., Goodwin, C.E.D., Robinson,
625 B.S., Hodgson, D.J. & Inger, R. (2018). A brief introduction to mixed effects modelling and multi-model
626 inference in ecology. *Peer J, 6,* 1–32.

627 Hill, R.A., & Hinsley, S.A. (2015). Airborne LiDAR for woodland habitat quality monitoring: Exploring
628 the significance of LiDAR data characteristics when modelling organism-habitat relationships. *Remote*
629 *Sensing*, *7*, 3446–3466.

630 Hill, R.A., Hinsley, S.A., Gaveau, D.L.A., & Bellamy, P.E. (2004). Cover: Predicting habitat quality for
631 great tits (*Parus major*) with airborne laser scanning data. *International Journal of Remote Sensing*,
632 *25*, 4851–4855.

633 Hyde, P., Dubayah, R., Peterson, B., Blair, J.B., Hofton, M., Hunsaker, C., & Walker, W. (2005).
634 Mapping forest structure for wildlife habitat analysis using waveform LiDAR: Validation of montane
635 ecosystems. *Remote sensing of Environment*, *96*, 427–437.

636 Hyde, P., Dubayah, R., Walker, W., Blair, J.B., Hofton, M., & Hunsaker, C. (2006). Mapping forest
637 structure for wildlife habitat analysis using multi-sensor (LiDAR, SAR/InSAR, ETM+, Quickbird)
638 synergy. *Remote Sensing of Environment*, *102*, 63–73.

639 Ibáñez-Álamo, J.D., Magrath, R.D., Oteyza, J.C., Chalfoun, A.D., Haff, T.M., Schmidt, K.A., Thomson,
640 R.L., & Martin, T.E. (2015). Nest predation research: Recent findings and future perspectives. *Journal*
641 *of Ornithology*, *156*, 247–262.

642 Klein, J., Haverkamp, P.J., Lindberg, E., Griesser, M., & Eggers, S. (2020). Remotely sensed forest
643 understory density and nest predator occurrence interact to predict suitable breeding habitat and the
644 occurrence of a resident boreal bird species. *Ecology and Evolution*, *10*, 2238–2252.

645 Koma, Z., Grootes, M.W., Meijer, C.W., Nattino, F., Seijmonsbergen, A.C., Sierdsema, H., Foppen, R.,
646 & Kissling, W.D. (2021). Niche separation of wetland birds revealed from airborne laser scanning.
647 *Ecography*, *44*, 907–918.

Kruuk, L.E.B., Osmond, H.L., & Cockburn, A. (2015). Contrasting effects of climate on juvenile body size in a Southern Hemisphere passerine bird. *Global Change Biology,* 21, 2929–2941.

Kubelka, V., Šálek, M., Tomkovich, P., Végvári, Z., Freckleton, R.P., & Székely, T. (2018). Global pattern of nest predation is disrupted by climate change in shorebirds. *Science*, *362*, 680–683.

Lahti, D.C. (2009). Why we have been unable to generalise about bird nest predation. *Animal Conservation*, *12*, 279–281.

Lefsky, M.A., Cohen, W.B., Parker, G.G., & Harding, D.J. (2002). LiDAR remote sensing for ecosystem studies: LiDAR, an emerging remote sensing technology that directly measures the three-dimensional distribution of plant canopies, can accurately estimate vegetation structural attributes and should be of particular interest to forest, landscape, and global ecologists. *BioScience*, *52*, 19–30.

Lima, S.L. (2009). Predators and the breeding bird: Behavioural and reproductive flexibility under the risk of predation. *Biological Reviews*, *84*, 485–513.

Lima, S.L., & Dill, L.M. (1990). Behavioural decisions made under the risk of predation: A review and prospectus. *Canadian Journal of Zoology*, *68*, 619–640.

Lüdecke, D., Ben-Shachar, M.S., Patil, I., Waggoner, P. & Makowski, D. (2021). performance: An R package for assessment, comparison, and testing of statistical models. *Journal of Open-Source Software, 6,* 3139.

Lv, L., Yang L., Osmond, H.L., Cockburn, A. & Kruuk, L.E.B. (2019). When to start and when to stop: Effects of climate on breeding in a multi-brooded songbird. *Global Change Biology, 26*, 443–457.

Lv, L., van de Pol, M., Osmond, H.L., Liu, Y., Cockburn, A., & Kruuk, L.E.B. (2022). Winter mortality of a passerine bird increases following hotter summers and during winters with higher maximum temperatures. *Science Advances*, in press.

Magrath, R.D., Haff, T.M., Horn, A.G., & Leonard, M.L. (2010). Calling in the face of danger: Predation risk and acoustic communication by parent birds and their offspring. In: Brockmann, H. J., Roper, T. J., Naguib, M., Wynne-Edwards, K. E., Mitani, J. C., & Simmons, L. W. (Eds.), Advances in the Study of Behaviour, pp. 187–253. Academic Press, London, UK.

Martin, T.E. (1993). Nest predation and nest sites. *BioScience*, *43*, 523–532.

675 Martin, T.E. (1998). Are microhabitat preferences of coexisting species under selection and adaptive?
676 *Ecology*, *79*, 656–670.

677 Martin, T.E., & Roper, J.J. (1988). Nest predation and nest-site selection of a western population of the
678 hermit thrush. *The Condor*, *90*, 51–57.

679 Matysioková, B., & Remeš, V. (2022). Stronger negative species interactions in the tropics supported by
680 a global analysis of nest predation in songbirds. *Journal of Biogeography*, *49*, 511–522.

681 Moran, P.A.P. (1950). Notes on continuous stochastic phenomena. *Biometrika, 37,* 17–23.

682 Mouton, J.C., & Martin, T.E. (2019). Nest structure affects auditory and visual detectability, but not
683 predation risk, in a tropical songbird community. *Functional Ecology*, *33*, 1973–1981.

684 Naef-Daenzer, B., & Grüebler, M.U. (2016). Post-fledging survival of altricial birds: Ecological
685 determinants and adaptation. *Journal of Field Ornithology*, *87*, 227–250.

686 Naef-Daenzer, B., Widmer, F., & Nuber, M. (2001). Differential post-fledging survival of great and coal
687 tits in relation to their condition and fledging date. *Journal of Animal ecology*, *70*, 730–738.

688 Nias, R. C. (1986). Nest-site characteristics and reproductive success in the superb fairy-wren. *Emu*, *86*,
689 139–144.

690 Prawiradilaga, D. M. (1996). Foraging ecology of pied currawongs *Strepera graculina* in recently
691 colonised areas of their range [PhD Thesis]. Australian National University.

692 R Core Team (2021). R: A language and environment for statistical computing. R Foundation for
693 Statistical Computing, Vienna, Austria.

694 Remeš, V., Matysioková, B., & Cockburn, A. (2012a). Long-term and large-scale analyses of nest
695 predation patterns in Australian songbirds and a global comparison of nest predation rates. *Journal of*
696 *Avian Biology*, *43*, 435–444.

697 Remeš, V., Matysioková, B., & Cockburn, A. (2012b). Nest predation in New Zealand songbirds: Exotic
698 predators, introduced prey and long-term changes in predation risk. *Biological Conservation*, *148*, 54–
699 60.

Reutebuch, S.E., Andersen, H.E., & McGaughey, R.J. (2005). Light detection and ranging (LIDAR): An emerging tool for multiple resource inventory. *Journal of Forestry*, *103*, 286–292.

Ricklefs R.E. (1969). An analysis of nesting mortality in birds. *Contributions to Zoology*, *9*, 1–48.

Roussel, J.R., Auty, D., Coops, N.C., Tompalski, P., Goodbody, T.R.H., Sánchez Meador, A., Bourdon, J.F., De Boissieu, F. & Achim, A. (2020). lidR: An R package for analysis of Airborne Laser Scanning (ALS) data. *Remote Sensing of Environment, 251*, 112061.

Rowley, I. & Russell, E.M. (1997). Fairy-wrens and grasswrens: Maluridae. Oxford University Press, Oxford, UK.

Sasaki, T., Imanishi, J., Fukui, W., & Morimoto, Y. (2016). Fine-scale characterization of bird habitat using airborne LiDAR in an urban park in Japan. *Urban Forestry and Urban Greening*, *17*, 16–22.

Schielzeth, H. (2010). Simple means to improve the interpretability of regression coefficients. *Methods in Ecology and Evolution, 1*, 103–113.

Segura, L.N., & Reboreda, J.C. (2012). Nest survival rates of red-crested cardinals increase with nest age in south-temperate forests of Argentina. *Journal of Field Ornithology*, *83*, 343–350.

Shokirov, S. (2021). Using multi-platform LiDAR to assess vegetation structure for woodland forest fauna [PhD Thesis]. Australian National University.

Shokirov, S., Jucker, T., Levick, S.R., Manning, A.D., Bonnet, T., Yebra, M., & Youngentob, K.N. (2023). Habitat highs and lows: Using terrestrial and UAV LiDAR for modelling avian species richness and abundance in a restored woodland. *Remote Sensing of Environment*, *285*, 113326.

Stoker, J. (2009). Visualization of multiple-return LiDAR data: Using voxels. *Photogrammetric Engineering and Remote Sensing*, *75*, 109–112.

Taylor, C.J., & Langmore, N.E. (2020). How do brood-parasitic cuckoos reconcile conflicting environmental and host selection pressures on egg size investment? *Animal Behaviour*, *168*, 89–96.

Taylor, M. (1992). Birds of the Australian Capital Territory: An Atlas. Canberra Ornithologists Group and National Capital Planning Authority, Canberra, Australia.

van Rees, E. (2013). Rapidlasso: Efficient tools for LiDAR processing. *GeoInformatics, 16,* 14–16.

726 Vehtari, A., Gelman, A., Simpson, D., Carpenter, B., & Bürkner, P.C. (2021). Rank-normalization,
727 folding, and localisation: An improved R-hat for assessing convergence of MCMC (with discussion).
728 *Bayesian Analysis*, *16*, 667–718.

729 Vierling, K.T., Swift, C.E., Hudak, A.T., Vogeler, J.C., & Vierling, L.A. (2014). How much does the time
730 lag between wildlife field-data collection and LiDAR-data acquisition matter for studies of animal
731 distributions? A case study using bird communities. *Remote sensing letters*, *5*, 185-193.

732 Vierling, K.T., Vierling, L.A., Gould, W.A., Martinuzzi, S., & Clawges, R.M. (2008). Lidar: Shedding new
733 light on habitat characterization and modelling. *Frontiers in Ecology and the Environment*, *6*, 90–98.

734 Woinarski, J.C., Braby, M.F., Burbidge, A.A., Coates, D., Garnett, S.T., Fensham, R.J., Legge, S.M.,
735 McKenzie, N.L., Silcock, J.L., & Murphy, B. P. (2019). Reading the black book: The number, timing,
736 distribution and causes of listed extinctions in Australia. *Biological Conservation*, *239*, 108261.

737 Woinarski, J.C., Stobo-Wilson, A.M., Crawford, H.M., Dawson, S.J., Dickman, C.R., Doherty, T.S.,
738 Fleming, P.A., Garnett, S.T., Gentle, M.N., Legge, S.M., Newsome, T.M., Palmer, R., Rees, M.W.,
739 Ritchie, E.G., Speed, J., Stuart, J.M., Thompson, E., Turpin, J., & Murphy, B.P. (2022). Compounding
740 and complementary carnivores: Australian bird species eaten by the introduced European red fox
741 *Vulpes vulpes* and domestic cat *Felis catus*. *Bird Conservation International*, *32*, 506–522.

742 Wood, K.A. (2000). Notes on the feeding habits of the pied currawong *Strepera graculina* at
743 Wollongong, New South Wales. *Australian Bird Watcher, 18,* 259–266.

744 Yasukawa, K., & Cockburn, A. (2009). Antipredator vigilance in cooperatively breeding superb fairy-
745 wrens (*Malurus cyaneus*). *The Auk*, *126*, 147–154.

746 Zuur, A.F., Ieno, E.N., Walker, N.J., Saveliev, A.A., & Smith, G.M. (2009). Mixed effects models and
747 extensions in ecology with R. Springer, New York, USA.

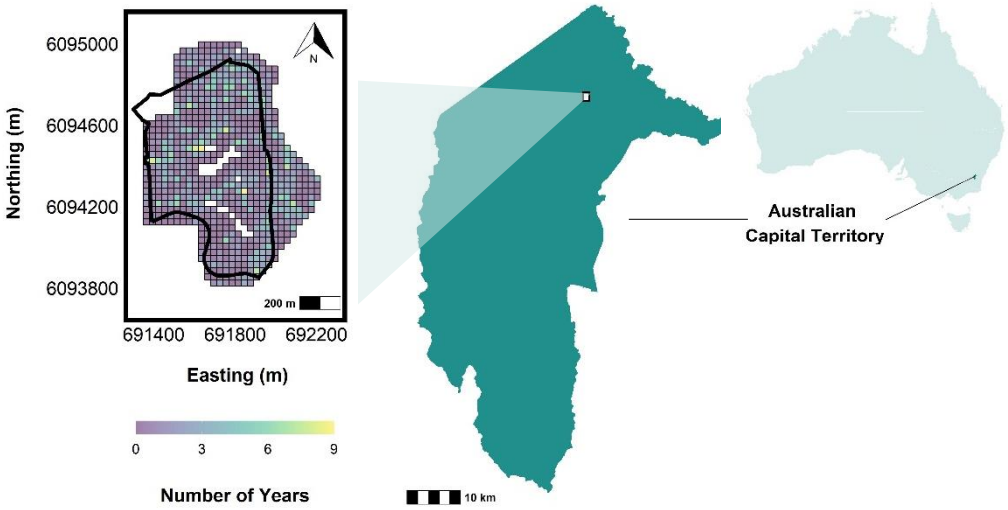

Figure 1: *Location of the study area in Canberra, Australian Capital Territory, Australia. The study area encompasses an area of c. 65 hectares that includes a managed area (c. 43 hectares) in the Australian National Botanic Gardens (ANBG; the perimeter of which is shown in black) and an unmanaged area (c. 22 hectares), which is part of the adjacent Black Mountain Nature Reserve. We established a 30 x 30 m resolution grid (n = 768 cells) over the extent of the study area, for which fairy-wren breeding data and ALS-derived vegetation structure parameters were extracted. Data for 27 of the 768 cells were excluded from analyses (shown in white), leaving a total of 741 cells; these excluded areas contain semi-artificial habitats that the fairy-wrens do not inhabit (see main text for further details). The left-hand panel shows the spatial distribution of the 741 cells across the study area, with cells shaded based on the number of years they contained a nest-site; the middle panel shows the location of the study area within the Australian Capital Territory; and the right-hand panel shows the latter's location in Australia.*

Table 1: *Overview of the understorey vegetation structure parameters derived from ALS for each 30 x 30 m resolution cell. z = normalised height value of LiDAR point; Voxel = A value of volume represented in three-dimensional (x, y, z) space.*

Parameter	**Parameter Abbreviation**	**Height Threshold**	**Description**	**Ecological Interpretation**
Mean height of the understorey vegetation (measured in metres)	Mean Height	0 – 8 m	Mean value of *z* within each 30 x 30 m resolution cell	A high mean height value indicates that a cell contains more tall shrubs and small trees, and fewer grass tussocks. A low mean height value indicates that a cell contains more grass tussocks and small shrubs. The spatial distribution of mean height across the study area is shown in Figure 2c.
Standard deviation of the height of the understorey vegetation (measured in metres)	SD Height	0 – 8 m	SD of *z* values within each 30 x 30 m resolution cell	SD height describes the variation in the vegetation height. A high SD height value indicates that a cell contains a more heterogenous, or complex, vegetation height distribution. The spatial distribution of SD height across the study area is shown in Figure 2d.
Volume of the vegetation in the lowest layer of the understorey (measured in cubic metres).	Groundstorey Volume	0 – 2 m	The number of 1 x 1 x 1 m voxels† between 0–2 m containing one or more vegetation point within each 30 x 30 m resolution cell. Maximum potential groundstorey volume is 1800 m^3 (i.e., 30 x 30 x 2 m).	The density of vegetation in the lowest understorey layer. The spatial distribution of groundstorey volume across the study area is shown in Figure 2e.

† Note: ALS point cloud data were converted to 1 x 1 x 1 m voxels using the voxelize_points function in the package 'lidR' (v.3.1.3; Rousel et al., 2020) in in R (v.4.0.5; R Core Team, 2021). The method of using voxels to estimate vegetation density followed e.g., Béland et al. (2014); Sasaki et al. (2016); Shokirov (2021), Shokirov et al. (2023); Stoker (2009).

Table 2: *Definition of terms and overview of the superb fairy-wren breeding parameters used in this study.*

Breeding Parameter	**Observation Level**	**Number of Observations**	**Description**	**Model Structure**
Nest Presence	A 30 x 30 m resolution cell in a given year (i.e., cell-year)	8151 cell-years (i.e., 741 cells; 11 years)	Cells that contained a nest in a given year were assigned a binary score of 1 (i.e., nest-cell-year) otherwise 0 (i.e., unused cell-year)	Bernoulli error distribution (and logit-link function)
Nest Success Rate	A nest-cell for a given breeding female in a given year (i.e., female-nest-cell-year)	1138 female-nest-cell-years	The number of successful nests relative to the total number of nest attempts for each breeding female in a nest-cell in a given year	Binomial error distribution (and logit-link function). The denominator (i.e., the total number of nest attempts for each female-nest-cell-year) was equal to 1 in 80.8% of observations
Fledgling Survival Rate	A nest-cell for a given breeding female in a given year (i.e., female-nest-cell-year)	556 female-nest-cell-years. Only female-nest-cell-years that contained one or more fledgling were included in this model	The number of fledglings to survive to independence relative to the total number of nestlings that successfully fledged for each breeding female in a nest-cell in a given year	Binomial error distribution (and logit-link function). In total, 22.1% of observations were zeros. Therefore, to account for excess zeros in the Binomial error distribution, we included a zero-inflated parameter in this model (Bürkner, 2017)
Reproductive Success	A nest-cell for a given breeding female in a given year (i.e., female-nest-cell-year)	1138 female-nest-cell-years	Female-nest-cell-years with one or more offspring successfully raised to independence were assigned a binary score of 1 (i.e., reproductive success) otherwise 0 (i.e., no reproductive success)	Bernoulli error distribution (and logit-link function)

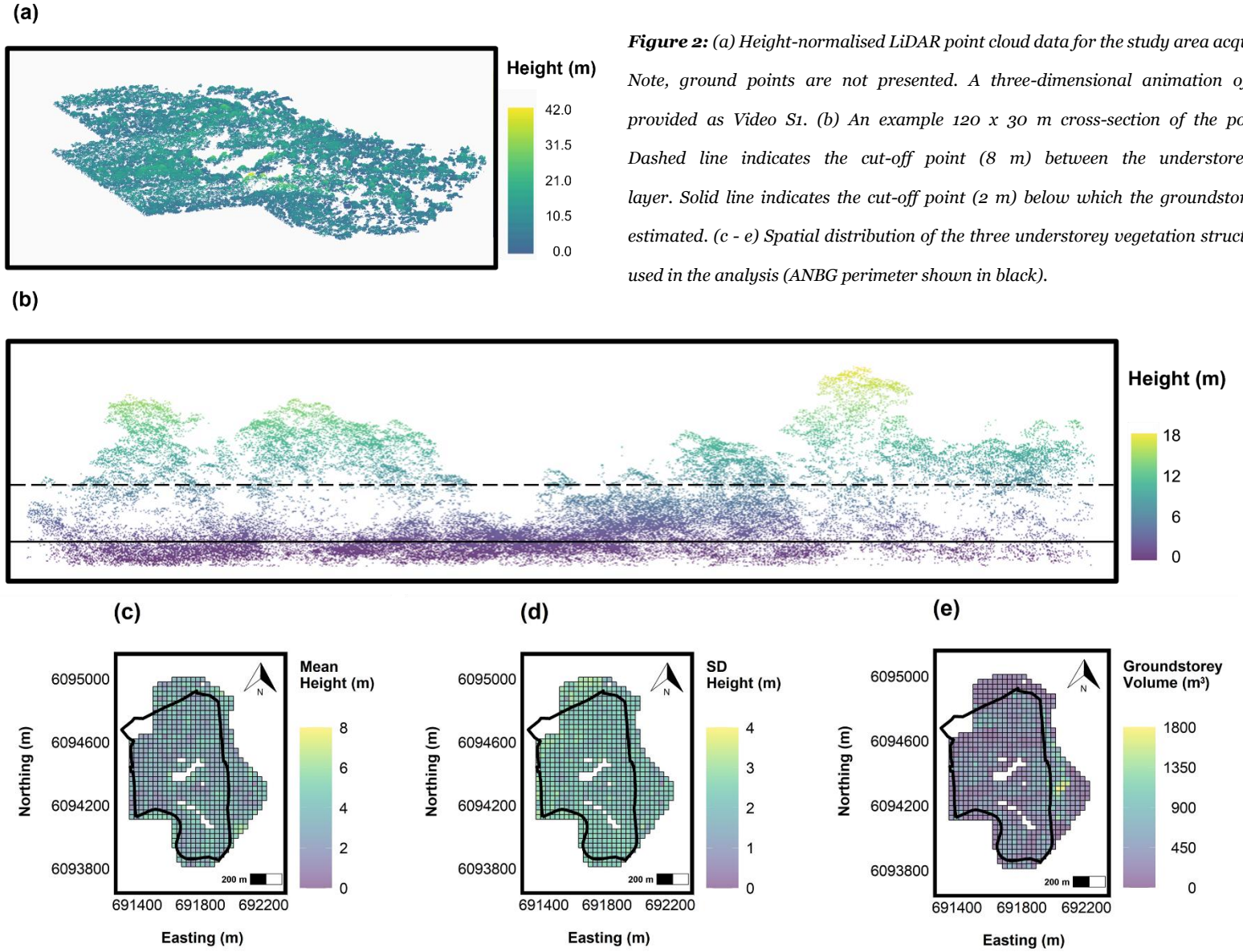

Figure 2: *(a) Height-normalised LiDAR point cloud data for the study area acquired using ALS. Note, ground points are not presented. A three-dimensional animation of these data is provided as Video S1. (b) An example 120 x 30 m cross-section of the point cloud data. Dashed line indicates the cut-off point (8 m) between the understorey and canopy layer. Solid line indicates the cut-off point (2 m) below which the groundstorey volume was estimated. (c - e) Spatial distribution of the three understorey vegetation structure parameters used in the analysis (ANBG perimeter shown in black).*

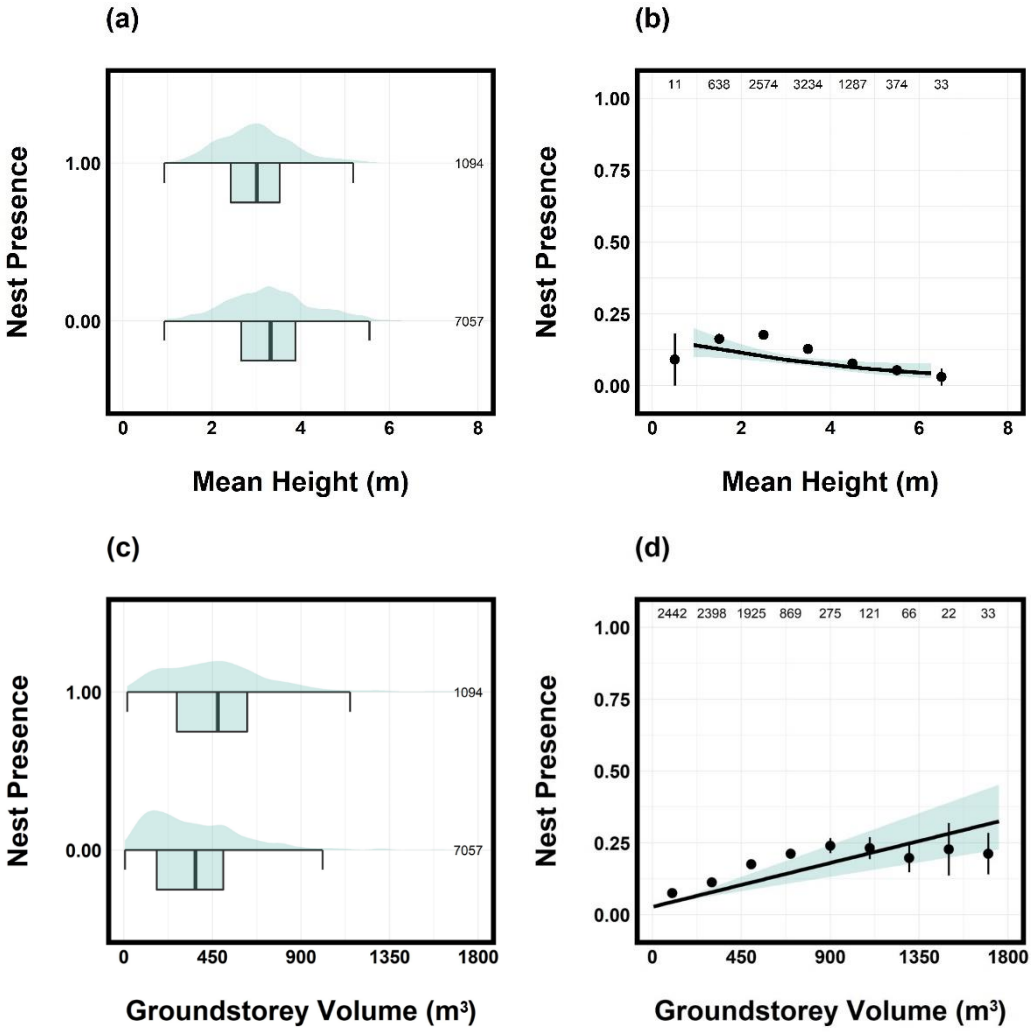

Figure 3: *Nest presence in relation to (a – b) mean height and (c – d) groundstorey volume. Panels (a) and (c) show the distribution of the raw data. The box and whiskers show the mean, plus upper and lower quartiles, and the interquartile range of the raw data for each group. Panels (b) and (d) show the model estimated marginal means (± 95% confidence intervals), after correcting for main effect parameters, as described in Methods. For visualisation purposes, the raw data were grouped into bins (each bin represents an interval of 1 m in (b) and an interval of 200 m³ in (d)) with points showing the group mean ± SE. In all panels, the number of observations (cell-years) in each group is given. Model estimates are provided in Table 3.*

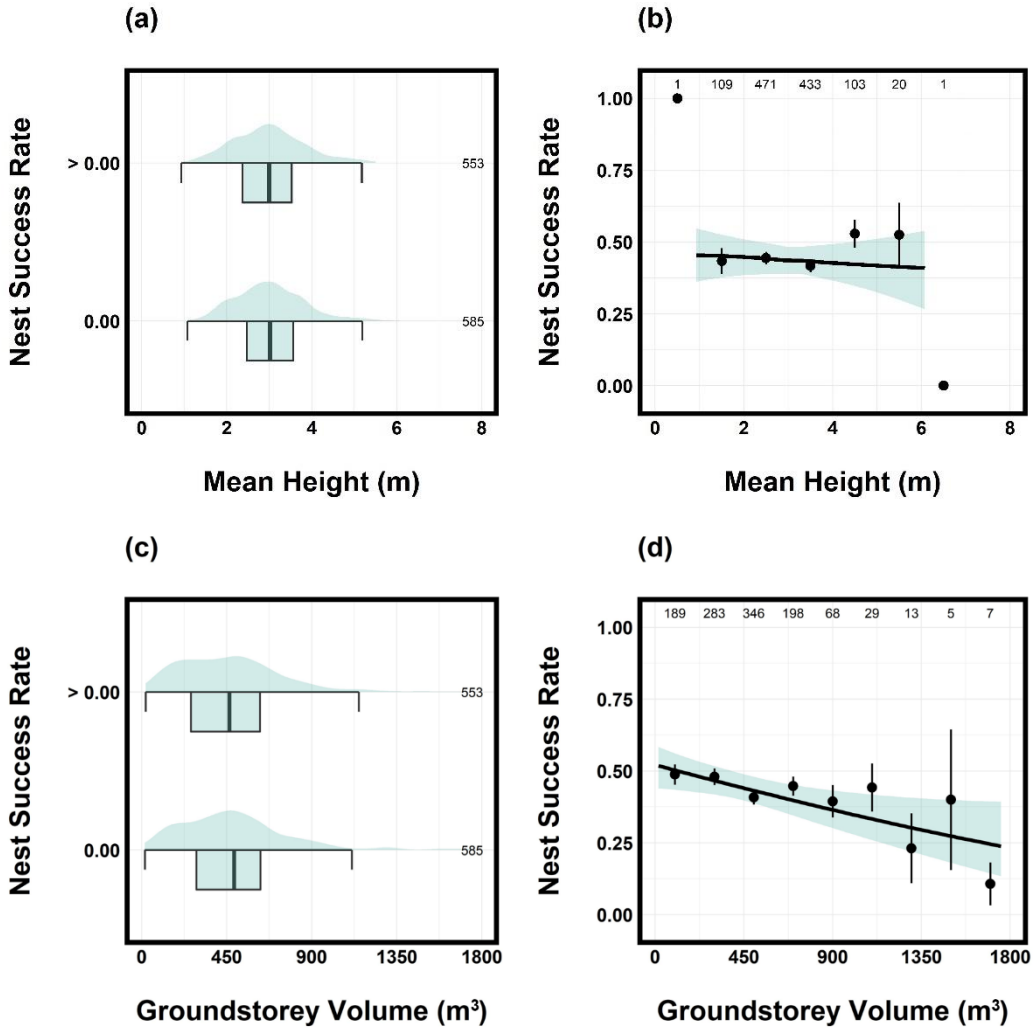

Figure 4: *Nest success rate in relation to (a – b) mean height and (c – d) groundstorey volume. Panels (a) and (c) show the distribution of the raw data. For visualisation purposes, the raw data were grouped into two bins: 0.00 and > 0.00. The box and whiskers show the mean, plus upper and lower quartiles, and the interquartile range of the raw data for each group. Panels (b) and (d) show the model estimated marginal means (± 95% confidence intervals), after correcting for main effect parameters, as described in Methods. For visualisation purposes, the raw data were grouped into bins (each bin represents an interval of 1 m in (b) and an interval of 200 m³ in (d)) with points showing the group mean ± SE. In all panels, the number of observations (female-nest-cell-years) in each group is given. Model estimates are provided in Table 3.*

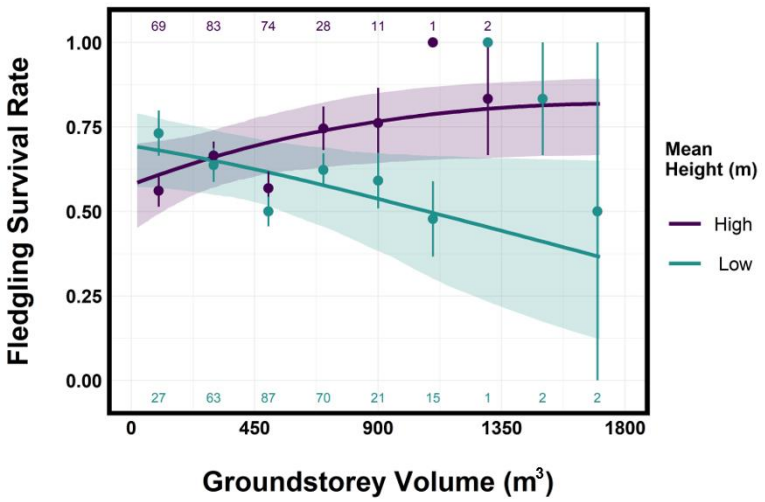

Figure 5: *Fledgling survival rate in relation to groundstorey volume when vegetation is low (green; mean height is less than the population-level average) or high (purple; mean height is greater than the population-level average). Regression lines show the model estimated marginal means (± 95% confidence intervals), after correcting for main effect parameters, as described in Methods. For visualisation purposes, the raw data were grouped into bins (each bin represents an interval of 200 m³) with points showing the group mean ± SE. The number of observations (female-nest-cell-years) in each group is given. Model estimates are provided in Table 3.*

Table 3: *Summaries of Bayesian spatial hierarchical generalised linear regression models. The parameter estimates are presented as posterior means ± standard deviation (SD) and 95% credible intervals (CI). All explanatory parameters were mean standardised for analysis. Main effect parameters for which the 95% CI do not overlap zero are highlighted in bold.*

Parameters	**Nest Presence** Estimate ± SD [95% CI]	**Nest Success Rate** Estimate ± SD [95% CI]	**Fledgling Survival Rate** Estimate ± SD [95% CI]	**Reproductive Success** Estimate ± SD [95% CI]
Intercept	**-2.37 ± 0.09 [-2.54 – -2.19]**	**-0.38 ± 0.13 [-0.63 – -0.12]**	**1.17 ± 0.24 [0.70 – 1.64]**	**-0.56 ± 0.15 [-0.86 – -0.29]**
Year	**-0.28 ± 0.07 [-0.43 – -0.13]**	0.04 ± 0.09 [-0.13 – 0.20]	0.05 ± 0.16 [-0.27 – 0.37]	0.05 ± 0.09 [-0.13 – 0.22]
Mean Height	**-0.24 ± 0.09 [-0.41 – -0.08]**	-0.04 ± 0.09 [-0.21 – 0.13]	0.24 ± 0.15 [-0.06 – 0.54]	0..03 ± 0.09 [-0.15 – 0.21]
SD Height	0.10 ± 0.07 [-0.04 – 0.25]	-0.04 ± 0.07 [-0.18 – 0.10]	-0.19 ± 0.13 [-0.44 – 0.05]	-0.13 ± 0.08 [-0.28 – 0.02]
Groundstorey Volume	**0.42 ± 0.08 [0.26 – 0.57]**	**-0.20 ± 0.07 [-0.33 – -0.06]**	0.07 ± 0.12 [-0.17 – 0.31]	-0.11 ± 0.08 [-0.27 – 0.04]
Groundstorey Volume: Mean Height	0.07 ± 0.07 [-0.06 – 0.20]	0.02 ± 0.07 [-0.11 – 0.16]	**0.34 ± 0.13 [0.10 – 0.59]**	0.10 ± 0.07 [-0.06 – 0.24]
Female Age (Relative to 1 Year Old)				
2+ Years Old		-0.02 ± 0.14 [-0.28 – 0.24]	-0.08 ± 0.21 [-0.50 – 0.33]	-0.10 ± 0.15 [-0.38 – 0.20]
Number of Helpers (Relative to 0)				
1+ Helpers		0.26 ± 0.13 [-0.01 – 0.51]	-0.07 ± 0.20 [-0.46 – 0.32]	**0.32 ± 0.14 [0.04 – 0.58]**
Random Effects	Variance Component ± SD [95% CI]	Variance Component ± SD [95% CI]	Variance Component ± SD [95% CI]	Variance Component ± SD [95% CI]
Cell ID	0.35 ± 0.19 [0.03 – 0.71]	0.19 ± 0.13 [0.01 – 0.49]	0.90 ± 0.18 [0.54 – 1.27]	0.22 ± 0.15 [0.01 – 0.55]
	(*n = 741*)	(*n = 448*)	(*n = 301*)	(*n = 448*)
Female ID		0.52 ± 0.11 [0.28 – 0.74]	0.81 ± 0.22 [0.33 – 1.24]	0.30 ± 0.15 [0.02 – 0.59]
		(*n = 317*)	(*n = 250*)	(*n = 317*)
Year	0.19 ± 0.08 [0.06 – 0.37]	0.13 ± 0.10 [0.01 – 0.36]	0.37 ± 0.17 [0.08 – 0.75]	0.16 ± 0.12 [0.01 – 0.44]
	(*n = 11*)	(*n = 11*)	(*n = 11*)	(*n = 11*)
Spatial Correlation	2.21 ± 0.23 [1.71 – 2.62]	0.17 ± 0.09 [0.01 – 0.39]	0.14 ± 0.11 [0.00 – 0.41]	0.16 ± 0.11 [0.01 – 0.43]
Zero Inflation Parameter			0.13 ± 0.02 [0.09 – 0.17]	
	n = 8151 cell-years	*n = 1138 female-nest-cell-years*	*n = 556 female-nest-cell-years*	*n = 1138 female-nest-cell-years*

Supplementary Information for:

Use of Airborne Laser Scanning to assess effects of understorey vegetation structure on nest-site selection and breeding performance in an Australian passerine bird

Richard S. Turner *, Ophélie J. D. Lasne, Kara Youngentob, Shukhrat Shokirov,

Helen L. Osmond, & Loeske E. B. Kruuk

* Corresponding author. Email: richard.turner@anu.edu.au

Supporting supplementary information included in this file is as follows:

Appendix S1: Supplementary Methods

Assessing spatial autocorrelation

Modelling data that relate to contiguous spatial regions, such as survey data, can pose a common problem in that they often display spatial autocorrelation (Dormann et al., 2007). In the case of our study, this would mean that cells from our 30 x 30 m resolution grid that were close together (i.e., neighbours) would likely be more similar in their understorey vegetation structure than those further apart. If spatial autocorrelation is present in the raw data and remains present in the residuals of the statistical model that uses such data, then inferences for that analyses will be violated. It is therefore important that researchers working with spatial data use diagnostic tools to check for spatial autocorrelation. In this study, we assessed for spatial autocorrelation for each of the three understorey vegetation structure parameters in each of our four datasets by calculating the Moran's *I* statistic (Moran, 1950), using the *moran.mc* function in the package 'spdep' (v.1.1.8; Bivand e*t al.,* 2013):

$$I = \frac{N \sum_{i=1}^{n} \sum_{j=1}^{n} w_{ij} (x_i - \bar{x})(x_j - \bar{x})}{(\sum_{i=1}^{n} \sum_{j=1}^{n} w_{ij}) \sum_{i=1}^{n} (x_i - \bar{x})^2} \quad \text{(a)}$$

Where N is the number of cells (N= 741 cells in our nest presence dataset, 448 cells in our nest success rate and reproductive success datasets, and 301 cells in our fledgling survival rate dataset), X_i and X_j are the understorey vegetation structure parameter values for cell i and j respectively, $\bar{x}$ is the mean of the understorey vegetation structure parameter across all cells, and W_{ij} is a spatial weights matrix of i relative to j. We used a binary spatial weights matrix, with W_{ij} equal to 1 if cells were identified as neighbours (otherwise 0). We identified neighbouring cells using a first order Queen's contiguity criterion – i.e., where common sides and common vertices are considered when defining the neighbour relation. This method differs from, for example, a first order Rook contiguity criterion, which considers only common sides when defining neighbour relations. Thus, where the Rook criterion will result in a cell having between 1–4 neighbours, the Queen criterion enables a cell to have up to eight neighbours.

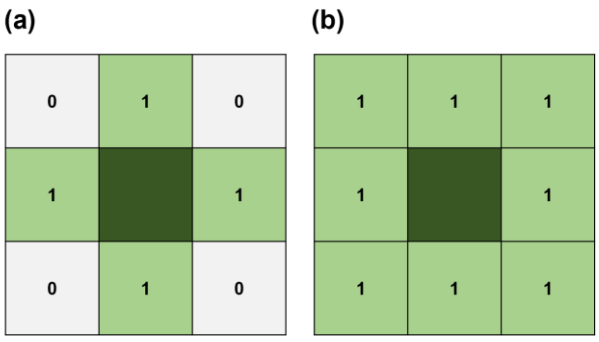

Example of the identification of neighbouring cells when using

(a) first order Rook contiguity criterion; (b) first order Queen's contiguity criterion.

These methods require all data to be contiguous. However, this was not the case for data in our nest success rate, fledgling survival rate, and reproductive success datasets, which were based on observations from a subset of our study area (Figure S9). Two cells in our nest success rate and reproductive success datasets, and seven cells in our fledgling survival rate dataset, contained no first order neighbours. Moreover, observations from larger sections of our study area were unlinked from either other. In cases where single observations were unlinked, we assigned them a single randomly chosen second order neighbour. In cases where larger sections of our study area were unlinked, we assigned one randomly chosen cell a randomly chosen second order neighbour, depicted below (Figure S9).

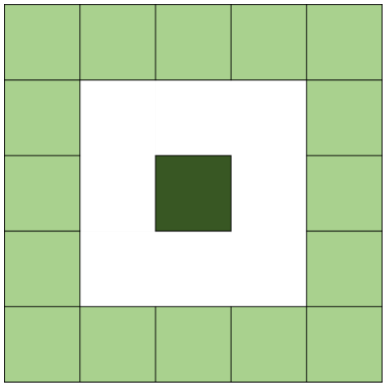

Cells that contained no first order neighbours were randomly assigned to one of a potential sixteen second order neighbours (light green).

Moran's *I* statistic ranges from −1.0 to 1.0. When *I* is positive, data are considered spatially clustered, whereas when *I* is negative data are considered spatially dispersed. When *I* is equal to 0 data are considered to be spatially random (Moran, 1950). Our diagnostics revealed that mean height, SD height, and groundstorey volume were all spatially clustered in the dataset that we used for our analysis of nest presence, and groundstorey volume was spatially clustered in the datasets that we used for our nest success rate and reproductive success models (Table S4, Figure S8). Therefore, we incorporated the spatial weights matrix as a conditional autoregressive (CAR) structure in all four of our models, to ensure the cell ID random effect was spatially structured.

Table S1: Summaries of Bayesian spatial hierarchical generalised linear regression models using the full breeding dataset from 1994–2019. The parameter estimates are presented as posterior means ± standard deviation (SD) and 95% credible intervals (CI). All explanatory parameters were mean standardised for analysis. Main effect parameters for which the 95% CI do not overlap zero are highlighted in bold.

Parameters	**Nest Presence** Estimate ± SD [95% CI]	**Nest Success Rate** Estimate ± SD [95% CI]	**Fledgling Survival Rate** Estimate ± SD [95% CI]	**Reproductive Success** Estimate ± SD [95% CI]
Intercept	**-2.06 ± 0.06 [-2.18 – -1.95]**	**-0.68 ± 0.08 [-0.84 – -0.52]**	**1.14 ± 0.15 [0.85 – 1.44]**	**-0.84 ± 0.09 [-1.01 – -0.66]**
Year	**-0.23 ± 0.05 [-0.32 – -0.13]**	**0.11 ± 0.04 [0.02 – 0.19]**	-0.06 ± 0.09 [-0.24 – 0.12]	0.06 ± 0.05 [-0.05 – 0.16]
Mean Height	**-0.14 ± 0.07 [-0.27 – -0.01]**	-0.00 ± 0.06 [-0.11 – 0.11]	0.09 ± 0.08 [-0.08 – 0.25]	0..03 ± 0.06 [-0.08 – 0.15]
SD Height	**0.13 ± 0.05 [0.03 – 0.23]**	-0.03 ± 0.04 [-0.12 – 0.05]	0.01 ± 0.07 [-0.12 – 0.14]	**-0.10 ± 0.05 [-0.19 – -0.01]**
Groundstorey Volume	**0.42 ± 0.08 [0.26 – 0.57]**	**-0.14 ± 0.05 [-0.24 – -0.05]**	0.05 ± 0.07 [-0.09 – 0.19]	**-0.10 ± 0.05 [-0.20 – -0.00]**
Groundstorey Volume: Mean Height	0.02 ± 0.05 [-0.08 – 0.12]	0.01 ± 0.05 [-0.08 – 0.10]	**0.20 ± 0.07 [0.07 – 0.34]**	0.06 ± 0.05 [-0.04 – 0.15]
Female Age (Relative to 1 Year Old)				
2+ Years Old		**0.23 ± 0.08 [0.07 – 0.39]**	-0.13 ± 0.12 [-0.36 – 0.11]	0.16 ± 0.09 [-0.01 – 0.34]
Number of Helpers (Relative to 0)				
1+ Helpers		**0.18 ± 0.08 [0.03 – 0.33]**	0.02 ± 0.11 [-0.19 – 0.23]	**0.22 ± 0.08 [0.06 – 0.38]**
Random Effects	Variance Component ± SD [95% CI]	Variance Component ± SD [95% CI]	Variance Component ± SD [95% CI]	Variance Component ± SD [95% CI]
Site ID	0.20 ± 0.13 [0.01 – 0.46]	0.37 ± 0.09 [0.16 – 0.53]	0.60 ± 0.11 [0.38 – 0.81]	0.37 ± 0.10 [0.15 – 0.54]
	(*n = 741*)	(*n = 627*)	(*n = 499*)	(*n = 627*)
Female ID		0.32 ± 0.09 [0.12 – 0.47]	0.71 ± 0.10 [0.51 – 0.90]	0.13 ± 0.09 [0.01 – 0.33]
		(*n = 731*)	(*n = 569*)	(*n = 731*)
Year	0.22 ± 0.04 [0.15 – 0.31]	0.10 ± 0.06 [0.01 – 0.23]	0.35 ± 0.08 [0.21 – 0.54]	0.16 ± 0.07 [0.02 – 0.30]
	(*n = 26*)	(*n = 26*)	(*n = 26*)	(*n = 26*)
Spatial Correlation	2.20 ± 0.13 [1.83 – 2.34]	0.20 ± 0.15 [0.01 – 0.53]	0.13 ± 0.09 [0.01 – 0.36]	0.15 ± 0.12 [0.01 – 0.46]
Zero Inflation Parameter			0.15 ± 0.01 [0.12 – 0.17]	
	n = 19266 cell-years	*n = 3148 female-nest-cell-years*	*n = 1443 female-nest-cell-years*	*n = 3148 female-nest-cell-years*

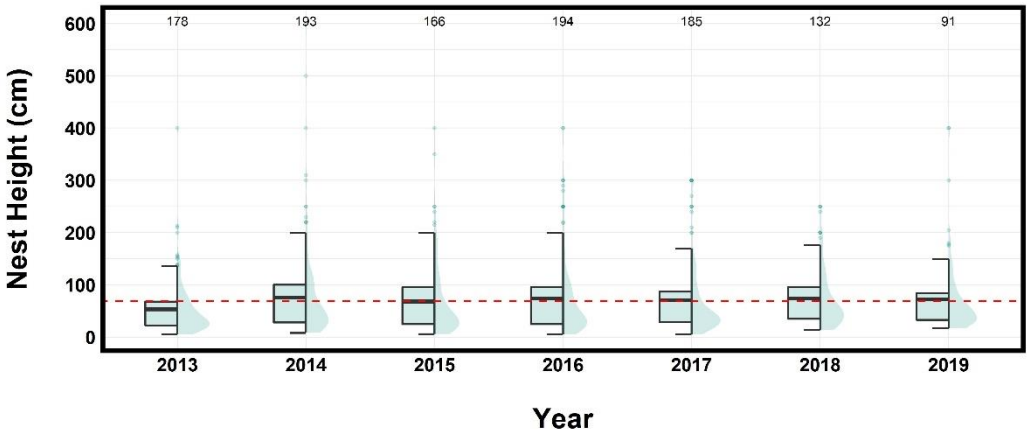

Figure S1: The height (cm) at which superb fairy-wrens built their nests in the study area (n = 1139 nests between 2013 – 2019, with 2013 being when we started recording nest height in our study area). For each year, the frequency distribution of the raw data is shown by the histogram, the box shows the mean, plus upper and lower quartiles, and the interquartile range, while the whiskers show the 95% confidence interval. The dashed red line is the mean nest height across all years. The number of nests in each year is given.

Nest locations between 2009 – 2019 (data used in this study):

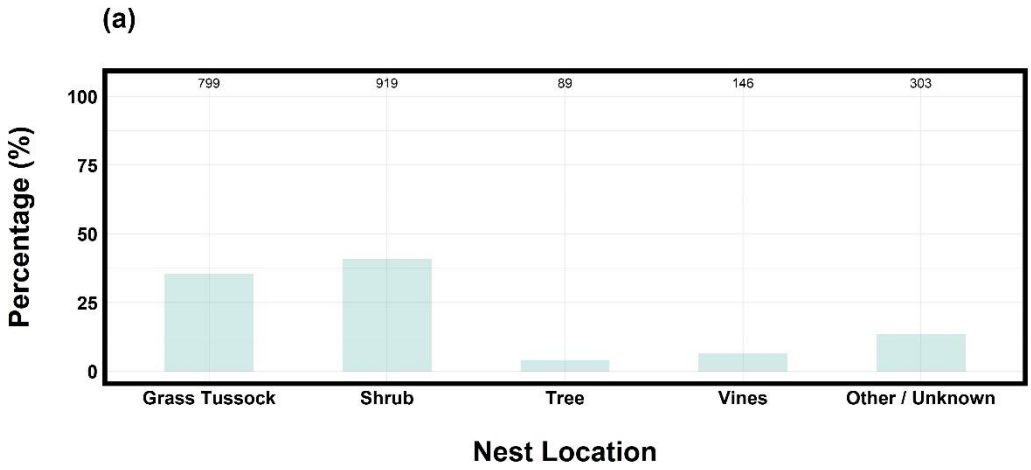

Nest locations between 1994 – 2019 (duration that comprehensive breeding data have been collected across the entire extent of the study area):

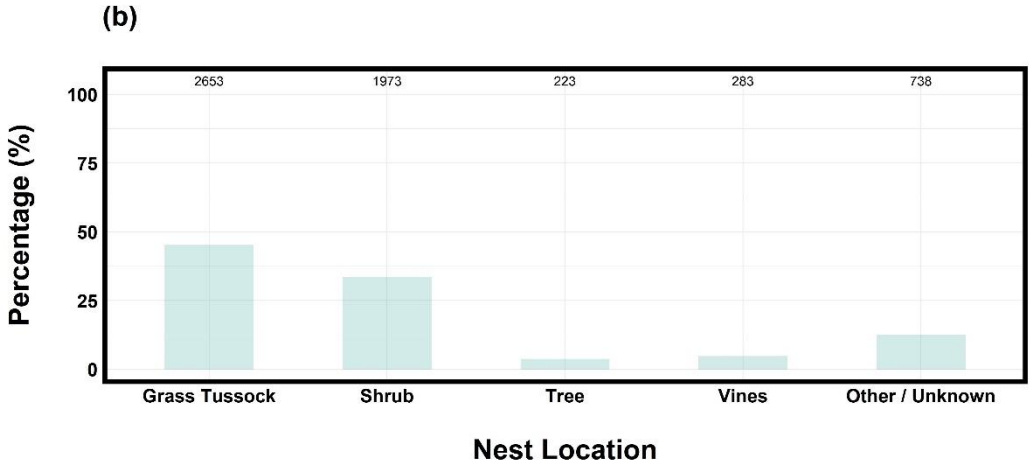

Figure S2: The percentage of superb fairy-wren nests built in different vegetation substrates in the study area (a) between 2009–2019; (b) between 1994–2019. The number of observations (number of nests) in each group is given.

Nest fate between 2009 – 2019 (data used in this study):

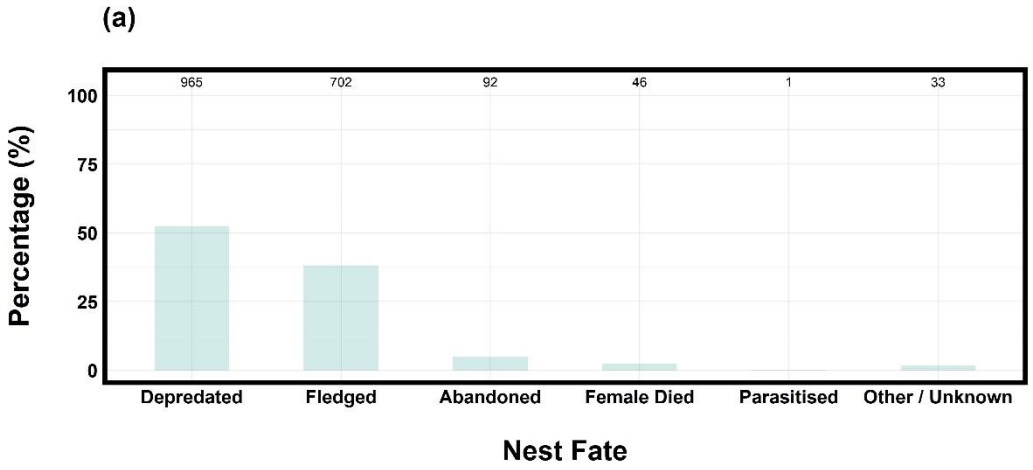

Nest fate between 1994 – 2019 (duration that comprehensive breeding data have been collected across the entire extent of the study area):

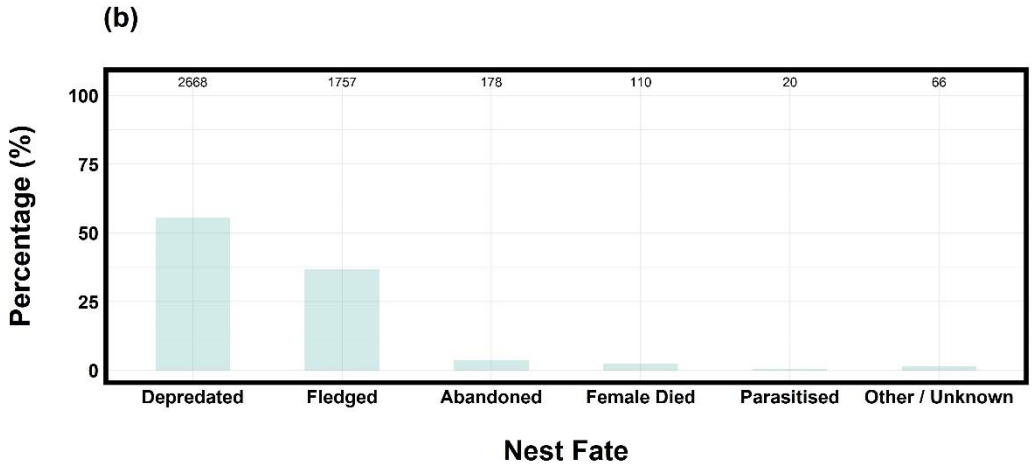

Figure S3: The fate of superb fairy-wren nests in the study area (a) between 2009 – 2019 (the years documented in this study, n = 1839 nests); (b) between 1994 – 2019 (the full duration of the study period, n = 4799). The number of observations (number of nests) in each group is given. Depredated = when all eggs or nestlings disappeared prior to their expected fledging date; *Fledged* = at least one offspring surviving to successfully fledge; *Abandoned* = nest failed after adult birds stopped incubating eggs or provisioning nestlings prior to their expected fledgling date; *Female died* = nest failed after the death of the breeding female; *Parasitised* = brood parasitised by cuckoos (e.g., see Turner et al., 2022); *Other / Unknown* = nest failed due to other or unknown cause.

Daily fledgling mortality rate between 2009 – 2019 (data used in this study):

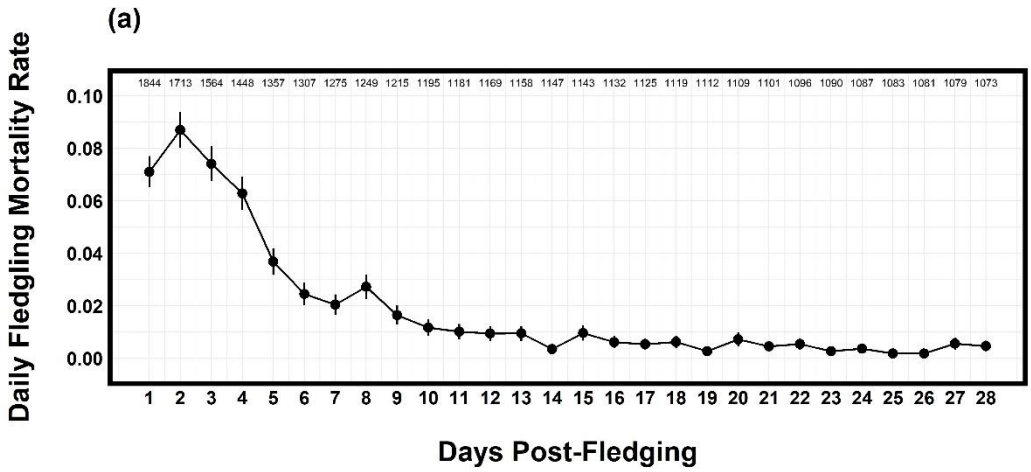

Daily fledgling mortality rate between 1994 – 2019 (duration that comprehensive breeding data have been collected across the entire extent of the study area):

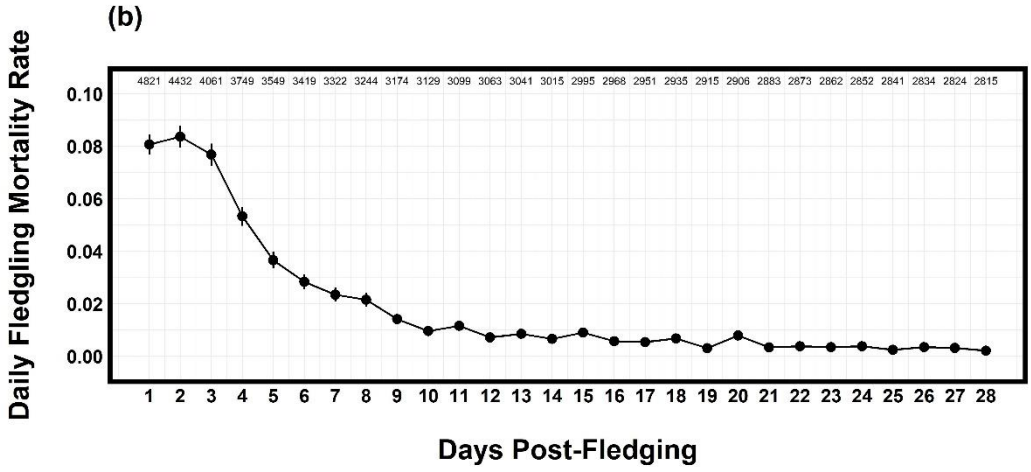

Figure S4: Mean (± SE) daily mortality rate of superb fairy-wren fledglings until independence (a) between 2009 – 2019 (n = 1844 fledglings); (b) between 1994 – 2019 (n = 4821 fledglings). The number of observations (fledgling-days) for each day is given.

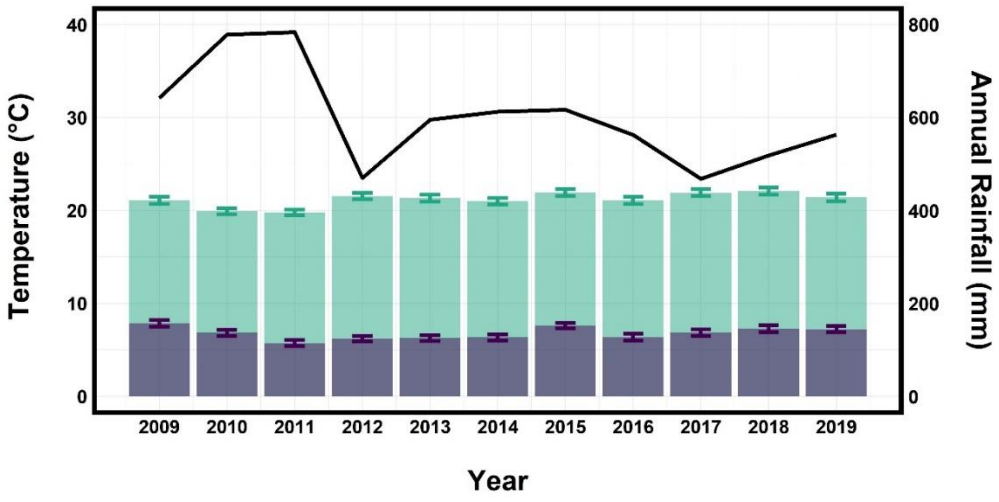

Figure S5: Mean (± SE) daily maximum (green bars) and minimum (purple bars) temperature, and total rainfall (black line) for each year of the study between 2009–2019. Note, a year spans 1 September – 31 August so, for example, 2019 consists of weather data from 1 September 2019–31 August 2020. Data were based on daily weather conditions at Canberra Airport, Australian Capital Territory, Australia (which is c. 8 km east of the study area) and were obtained from the Australian Bureau of Meteorology (http://www.bom.gov.au/climate/data).

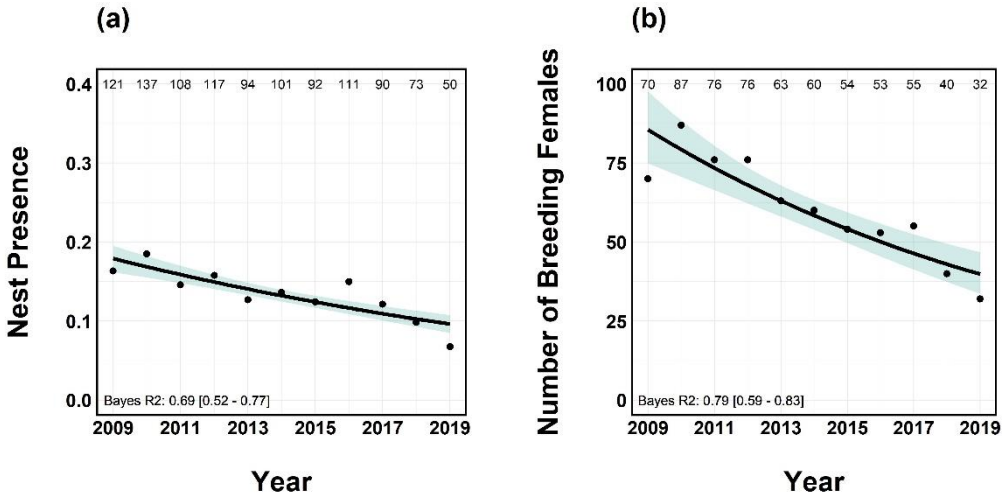

Figure S6: The change in (a) nest presence; (b) the number of breeding females in the study area over time. is. The regression lines represent model estimated marginal means (± 95% confidence intervals) from simple linear regressions. The number of observations (in (a) the number of cells with a nest; in (b) number of breeding females) in each year is given across the top of each graph.

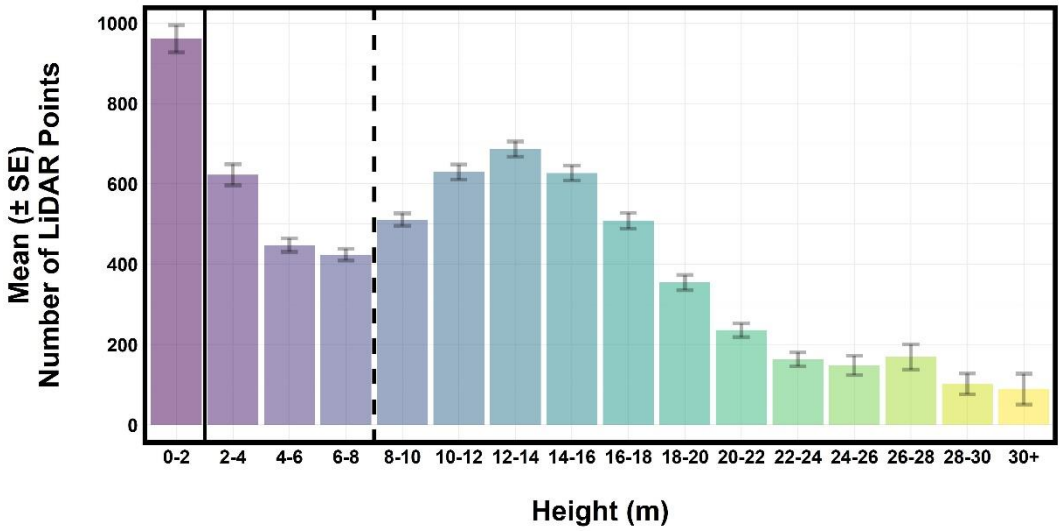

Figure S7: Mean (± SE) number of LiDAR vegetation points in each cell (n = 741) at 2 metre height increments. Dashed line indicates the chosen cut-off point (8 m) between the understorey and canopy layer. Solid line indicates the chosen cut-off point (2 m) at which the groundstorey volume was estimated.

Table S2: Checking for multicollinearity among model parameters. The Variance Inflation Factor (VIF) is calculated as 1/(1 – R^2); values < 5 indicate a low correlation between the parameter and other model parameters. The Increased SE indicates how much larger the standard error is the parameter due to associations with other model parameters. Tolerance is calculated as 1/VIF, and indicates the amount of variability in the parameter that is not explained by the other model parameters. Multicollinearity checks were implemented using the check_collinearity function in the R package 'performance' (v.0.7.2; Lüdecke et al., 2021).

Nest Presence			
Parameters	VIF	Increased SE	Tolerance
Year	1.00	1.00	1.00
Mean Height	1.54	1.24	0.65
SD Height	1.19	1.09	0.84
Groundstorey Volume	1.53	1.24	0.65
Groundstorey Volume: Mean Height	1.44	1.20	0.69

Nest Success Rate			
Parameters	VIF	Increased SE	Tolerance
Year	1.03	1.02	0.97
Mean Height	1.95	1.40	0.51
SD Height	1.34	1.16	0.75
Groundstorey Volume	1.32	1.15	0.76
Groundstorey Volume: Mean Height	1.44	1.20	0.69
Mother Age	1.04	1.02	0.96
Number of Helpers	1.05	1.02	0.95

Fledgling Survival Rate			
Parameters	VIF	Increased SE	Tolerance
Year	1.01	1.01	0.99
Mean Height	2.09	1.45	0.48
SD Height	1.23	1.11	0.81
Groundstorey Volume	1.24	1.11	0.81
Groundstorey Volume: Mean Height	1.57	1.25	0.64
Mother Age	1.02	1.01	0.98
Number of Helpers	1.02	1.01	0.98

Reproductive Success			
Parameters	VIF	Increased SE	Tolerance
Year	1.03	1.02	0.97
Mean Height	1.88	1.37	0.53
SD Height	1.28	1.13	0.78
Groundstorey Volume	1.23	1.11	0.81
Groundstorey Volume: Mean Height	1.41	1.19	0.71
Mother Age	1.08	1.04	0.92
Number of Helpers	1.07	1.04	0.93

*Table S3: Pearson coefficients indicating the level of relationship between main effect parameters in each of the four Bayesian spatial hierarchical regression models: (**a**) nest presence; (**b**) nest success rate; (**c**) fledgling survival rate; (**d**) Reproductive Success. Positive relationships are highlighted in green, whilst negative relationships are in purple. Shading is dependent on the strength of the relationship, becoming bolder as relationships approach +1 or -1.*

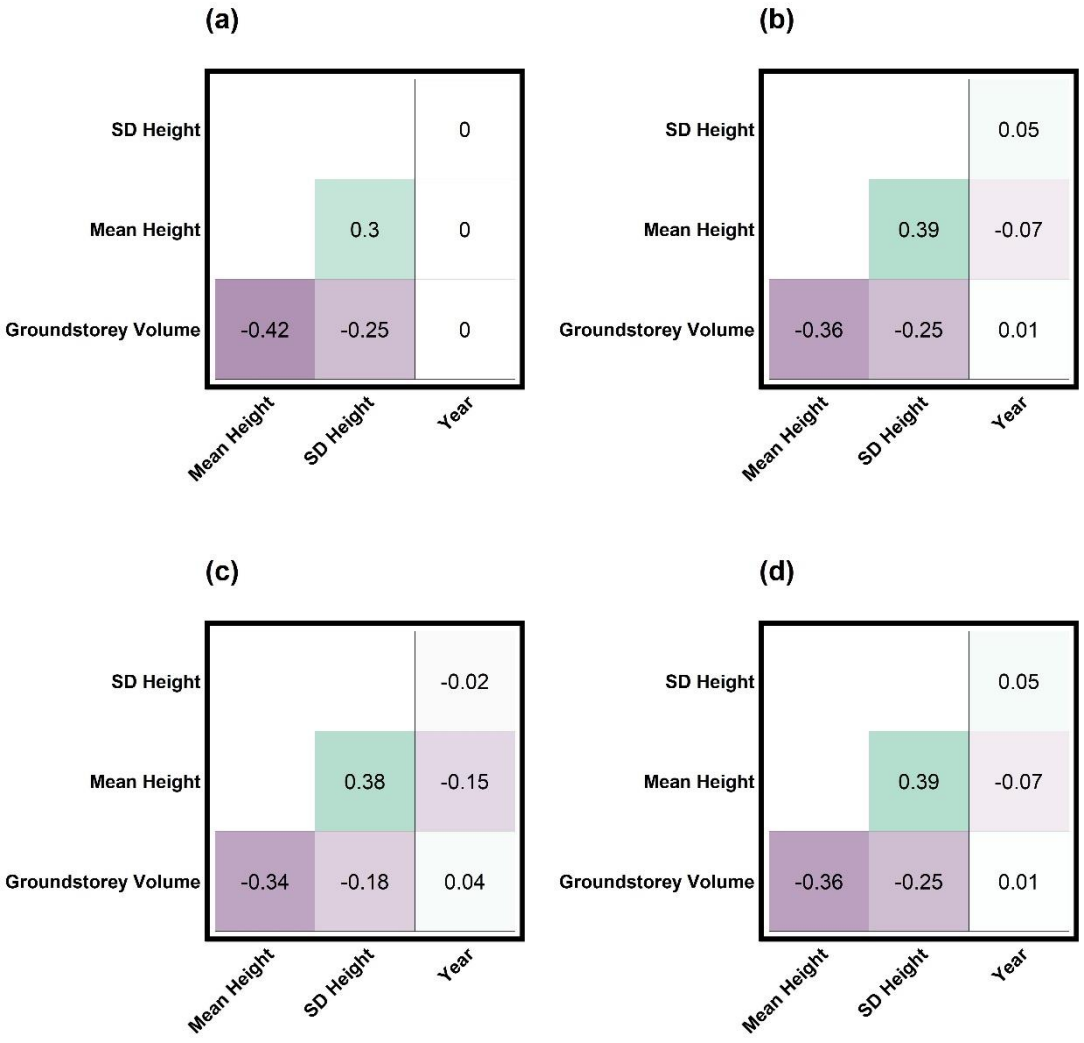

Table S4: Checking for spatial autocorrelation among understorey vegetation structure parameters. Spatial autocorrelation was considered significant when pseudo-P < 0.05 (highlighted in bold). Moran's I statistics were calculated using the moran.mc function in the R package 'spdep' (v.1.1.8; Bivand et al., 2013).

Nest Presence		
Parameters	Moran's *I*	Pseudo-P
Mean Height	0.29	< **0.001**
SD Height	0.26	< **0.001**
Groundstorey Volume	0.48	< **0.001**
Number of Cells (n = 741)		
Mean Number of Neighbours/Cells (n = 7.34)		
Number of Monte-Carlo Simulations (n = 2000)		

Nest Success Rate		
Parameters	Moran's *I*	Pseudo-P
Mean Height	0.04	0.07
SD Height	0.04	0.10
Groundstorey Volume	0.05	**0.05**
Number of Cells (n = 448)		
Mean Number of Neighbours/Cells (n = 5.17)		
Number of Monte-Carlo Simulations (n = 2000)		

Fledgling Survival Rate		
Parameters	Moran's *I*	Pseudo-P
Mean Height	0.01	0.38
SD Height	-0.03	0.76
Groundstorey Volume	0.03	0.18
Number of Cells (n = 301)		
Mean Number of Neighbours/Cells (n = 3.86)		
Number of Monte-Carlo Simulations (n = 2000)		

Reproductive Success		
Parameters	Moran's *I*	Pseudo-P
Mean Height	0.04	0.07
SD Height	0.04	0.10
Groundstorey Volume	0.05	**0.05**
Number of Cells (n = 448)		
Mean Number of Neighbours/Cells (n = 5.17)		
Number of Monte-Carlo Simulations (n = 2000)		

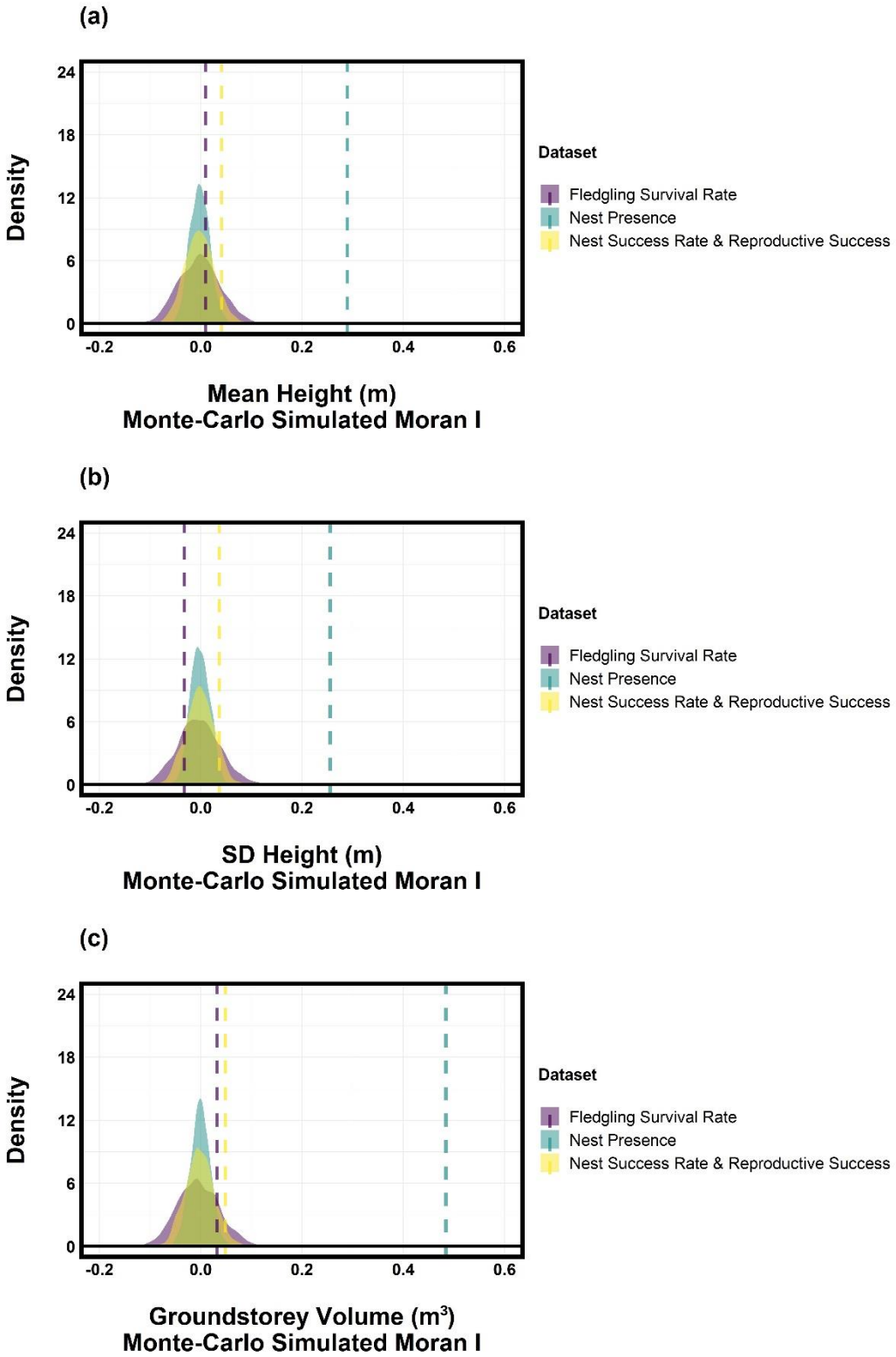

Figure S8: Density plots of Monte-Carlo simulated Moran's I statistics (n = 2000 simulations) for (a) mean height; (b) SD height; and (c) groundstorey volume in each dataset. The curve shows the distribution of expected Moran's I if the understorey vegetation structure parameters were randomly distributed. The dashed line indicates the observed Moran's I. Moran's I statistics were calculated using the moran.mc function in the R package 'spdep' (v.1.1.8; Bivand et al., 2013).

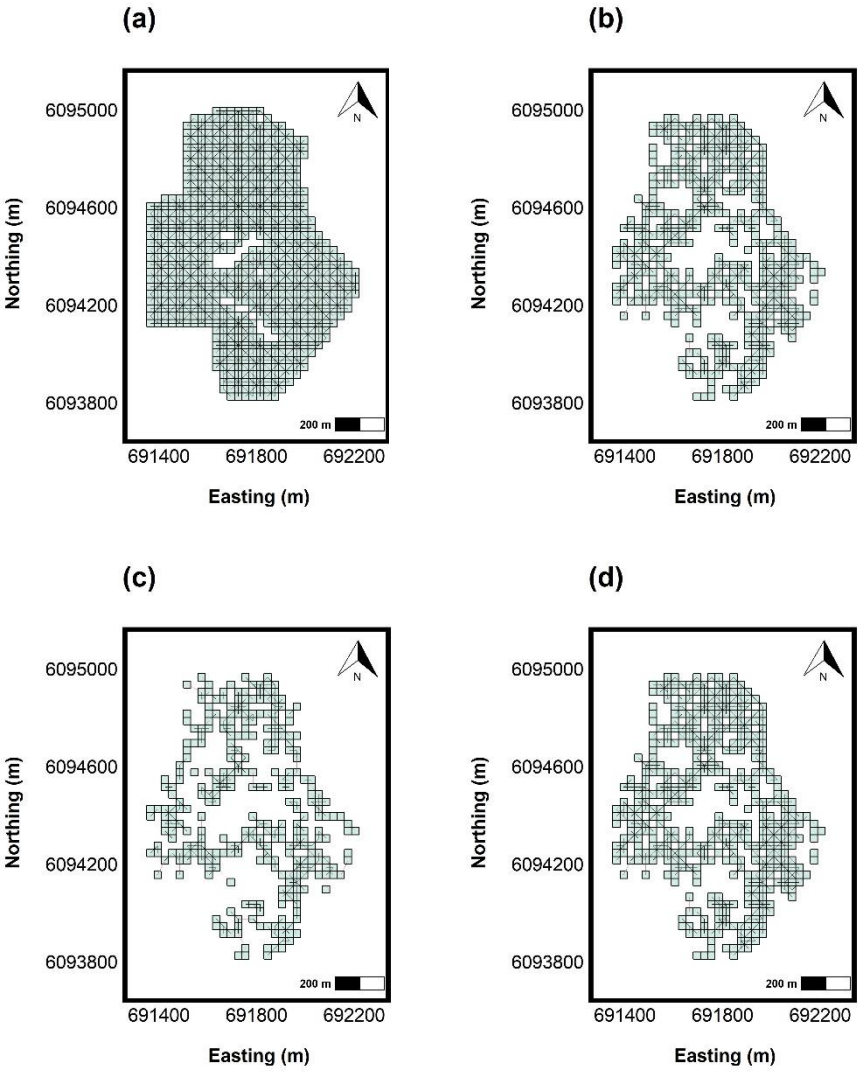

Figure S9: Visualisation of the spatial weights matrix used in each of our four Bayesian spatial hierarchical generalised linear models: (a) nest presence (n = 741 cells; mean number of neighbours = 7.34); (b) nest success rate (n = 449 cells; mean number of neighbours = 5.18); (c) fledgling survival rate (n = 301 cells; mean number of neighbours = 3.86); (d) Reproductive Success (n = 449 cells; mean number of neighbours = 5.18). Shown in red are the links that were randomly chosen to ensure our data were contiguous.

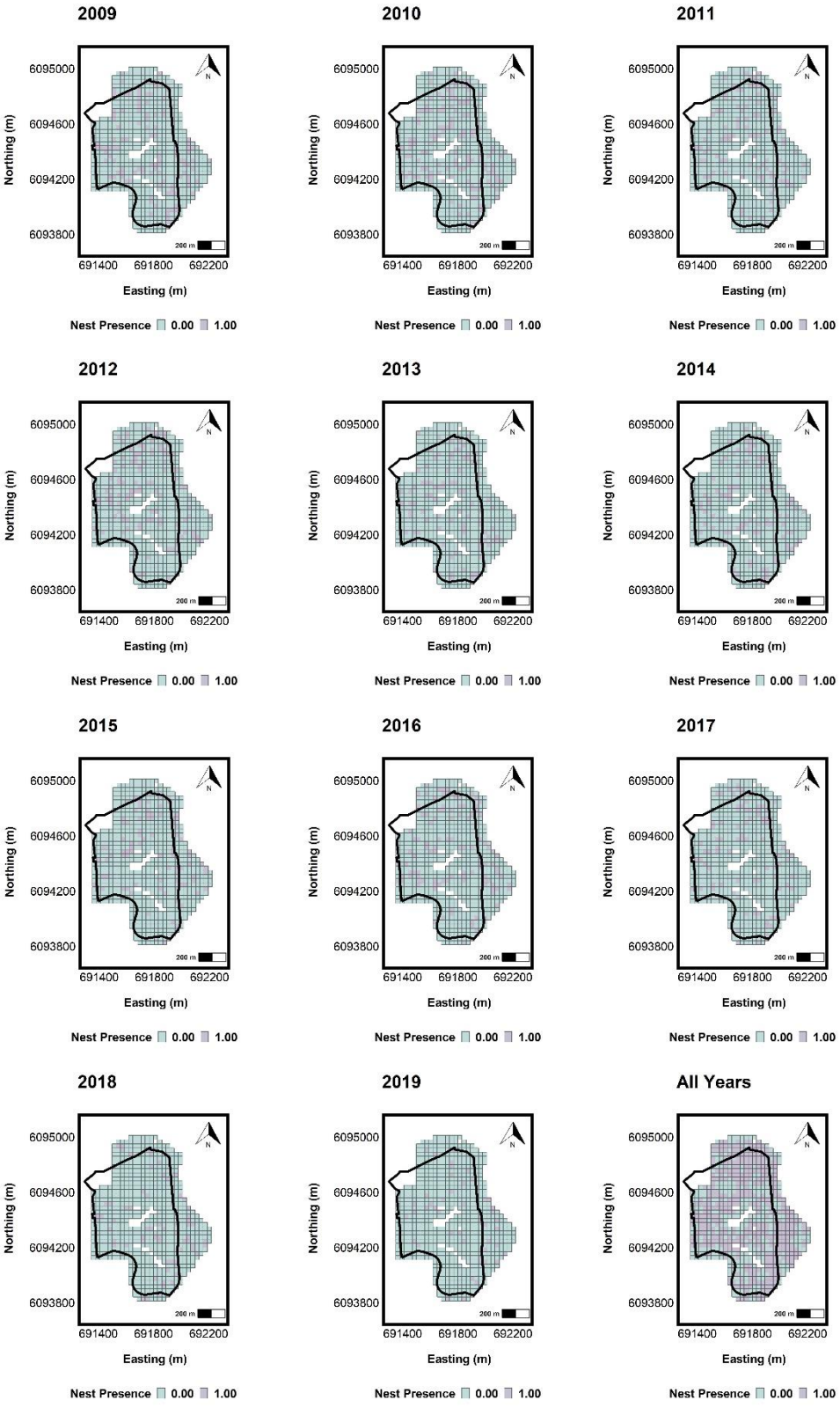

Figure S10: Spatiotemporal distribution of superb fairy-wren nest-sites in the study area (between 2009–2019).

References

Bivand, R.S., Pebesma, E. & Gomez-Rubio, V. (2013). *Applied spatial data analysis with R (2nd edition)*. Springer, New York.

Dormann, C. F., McPherson, J. M., Araújo, M. B., Bivand, R., Bolliger, J., Carl, G., Davies, R. G., Hirzel, A., Jetz, W., Kissling, W. D., Kühn, I., Ohlemüller, R., Peres-Neto, P. R., Reineking, B., Schröder, B., Schurr, F. M., & Wilson, R. (2007). Methods to account for spatial autocorrelation in the analysis of species distributional data: A review. *Ecography*, *30*, 609–628.

Lüdecke, D., Ben-Shachar, M.S., Patil, I., Waggoner, P. & Makowski, D. (2021). performance: An R package for assessment, comparison, and testing of statistical models. *Journal of Open Source Software, 6,* 3139.

Moran, P.A.P. (1950). Notes on continuous stochastic phenomena. *Biometrika, 37,* 17–23.

Turner, R.S., Langmore, N.E., Osmond, H.L., & Cockburn, A. (2022). First recorded evidence of ejection of a cuckoo egg in a fairy-wren species. *Australian Field Ornithology, 39,* 104–109.